J. Fluid Mech. (1998), *vol.* 357, *pp.* 289–320. Printed in the United Kingdom

On the complete radiation–diffraction problem and wave-drift damping of marine bodies in the yaw mode of motion

By STYRK FINNE AND JOHN GRUE

Mechanics Division, Department of Mathematics, University of Oslo, Norway

(Received 16 May 1997 and in revised form 30 October 1997)

The coupled radiation–diffraction problem due to a floating body with slow (time-dependent) rotation about the vertical axis in incoming waves is studied by means of potential theory. The water depth may be finite. First, the radiation problem is described. It is shown how the various components of the velocity potential may be obtained by means of integral equations. The first-order forces in the coupled radiation–diffraction problem are then considered. Generalized Haskind relations for the exciting forces and generalized Timman–Newman relations for the added mass and damping forces are deduced for bodies of arbitrary shape with vertical walls at the water line. The equation of motion is obtained, and the frequencies of the linear body responses superposed on the slow rotation are identified. Formulae for the wave-drift damping coefficients in the yaw mode of motion are derived in explicit form, and the energy equation is discussed. Computations illustrating the various aspects of the method are performed for two ships. The wave-drift damping moment is found to become positive in the present examples. When the rotation axis is moved far away from the body, the slow motion becomes effectively unidirectional, and results of the translational case are recovered.

1. Introduction

The coupled radiation–diffraction problem due to a floating body moving with a slow rotation about the vertical axis in monochromatic waves is considered. The paper is complementary to the work by Grue & Palm (1996) who described the corresponding diffraction problem. The radiation problem is outlined in the first few sections of the paper. In this case, a body is performing forced small oscillations in six degrees of freedom superimposed on a slow rotation about the vertical axis in the surface of an otherwise calm fluid. The coupled radiation–diffraction problem is considered next, as we derive formulae for the induced hydrodynamical forces and the equation of motion determining the linear body responses. The ultimate goal is to describe the remaining parts of a method to obtain the three-by-three wave-drift damping matrix of a floating body of general shape, including the complete radiation–diffraction effects.

The study is motivated by needs in the offshore industry to describe wave-induced forces on and motions of moored production ships and floating oil platforms. Such production systems may be lightly moored and may experience slow motions with large amplitudes in the horizontal plane. These motions are excited by nonlinear loads due to wind, current and waves, and have periods determined by the mass and

spring properties of the moored body. They are limited by hydrodynamical damping forces, where wave-drift damping has proved to make an important contribution.

The notion of wave-drift damping was introduced by Wichers & van Sluijs (1979) who performed decaying tests for moored tankers in waves. Rational theories were derived after some while, enabling the evaluation of wave-drift damping due to a slow translation, by Huijsmans & Hermans (1985), Zhao & Faltinsen (1989), Nossen, Grue & Palm (1991), Grue & Palm (1993) for bodies of arbitrary shape, and by Emmerhoff & Sclavounos (1992), Malenica, Clark & Molin (1995) for vertical circular cylinders. Later, wave-drift damping due to a slow rotation was accounted for by Newman (1993), who also considered the complete wave-drift damping matrix, and by Grue & Palm (1996). The latter two works allow for arbitrary geometries, but the problem is simplified by considering only the diffraction part of the linear wave field in infinite water depth. Wave-drift damping in the yaw mode of motion is also described for vertical circular cylinders by Emmerhoff & Sclavounos (1996).

A realistic wave environment at sea contains several frequency components and may also be multidirectional. Here we shall assume that the sea is longcrested which represents a first step of simplification. This assumption is also of relevance to many sea states. The leading part of the nonlinear wave force contains components that are proportional to the square of the characteristic wave amplitude and oscillate with frequencies corresponding to the sum and difference between each pair of the frequencies, ω_j and ω_k, say, of the wave spectrum. Here we focus on the components of the low-frequency force $\mathrm{Re}\{F(\omega_j, \omega_k)\exp(\mathrm{i}(\omega_j - \omega_k)t)\}$. If the resonance frequency of the oscillating system is low, or the wave spectrum is narrow-banded, we may apply the Newman approximation, which means that $F(\omega_j, \omega_k)$ is replaced by $F(\omega_j, \omega_j)$. This significantly simplifies the mathematical problem since we may analyse the force due to each wave component separately and combine the effect due to the various wave components subsequently. The theory outlined below, under the assumption of incoming monochromatic unidirectional waves, is applicable to irregular seas in this context.

In the present work we describe the complete radiation–diffraction problem of a floating body of arbitrary shape rotating slowly about the vertical axis, generalizing the method by Grue & Palm (1996, hereinafter referred to as GP). We apply potential theory to describe the motion of an incompressible and homogeneous fluid, as viscous effects are disregarded (§§ 2–3). The mathematical problem is formulated in the relative frame of reference following the slow rotation of the body. The water depth is allowed to be finite in all derivations. Applying perturbation expansions in the wave amplitude and the slow angular velocity we decompose the velocity potential, deriving a set of boundary value problems for its various components. The coupling between the slow motion and steady second-order velocities in the fluid is consistently accounted for (§ 4). The boundary value problems are solved by means of integral equations involving unknown quantities on the wetted body surface only (§ 5). The method requires evaluation of ordinary integrals over the mean free surface, which have relatively quick convergence and are relatively robust to evaluate.

In § 6 the first-order forces and motions of the body are considered. Several results customary in the case of unidirectional motion of a body in waves may be generalized to the case of a slow rotation of the body, still allowing for a general shape of the geometry, except for a requirement of vertical walls at the water line. Thus we deduce generalized Haskind relations for the exciting forces and generalize the Timman–Newman relations for the added mass and damping forces to the present case. Numerical results confirm these relations. The equation of motion determining

the linear responses of the body is derived, accounting for the Coriolis force. We also identify the frequencies of the linear body responses which are superimposed on the slow rotation, finding that the different modes of motion may in general have different frequencies. Furthermore, the frequency of the motion may differ from the frequency of the exciting force in the respective modes.

Formulae for the wave-drift damping coefficients due to the slow rotation (§ 7) are derived in explicit form using conservation of linear and angular momentum. The derivations in the coupled radiation–diffraction problem become somewhat more complex than when there are no body responses. The resulting formulae are compared with the diffraction analyses by Newman (1993), GP and Grue (1996). Wave-drift damping computations are performed for two ships. The wave-drift damping moment is found to become positive in the present examples. We also compare wave-drift damping, which grows with the wave amplitude squared, and viscous damping in the yaw mode, finding that the former may dominate even for small wave amplitude (§ 7.4). Various aspects of the method are discussed in § 8, including convergence and energy balance. The convergence tests indicate that the linear forces and motions, the time-averaged second-order forces and the wave-drift damping matrix may be obtained with a relative accuracy of a few percent, depending on the discretization of the geometry.

For a slow rotation about a vertical axis far away from the body we recover results due to a slow unidirectional motion. In this connection, it is relevant to compare some recent formulae for the translatory problem proposed by Aranha (1996). We find a general disagreement between our method and his, both for the linear and second-order parts of the problem; the details are explained in § 8. Finally, § 9 is a conclusion.

2. Mathematical formulation

We consider a floating body moving with a slow yaw velocity (rotation about the vertical axis) while responding to incoming monochromatic waves. We define a fixed frame of reference and a relative frame of reference where the latter follows the slow motion of the body, which is rotated an angle α relative to the fixed frame of reference. A coordinate system $Oxyz$ is introduced in the relative frame of reference with the (x, y)-plane in the mean free surface of the fluid and the z-axis vertical upwards. Unit vectors $\boldsymbol{i}, \boldsymbol{j}, \boldsymbol{k}$ are introduced accordingly. The angular velocity is denoted by $\Omega\boldsymbol{k} = \dot{\alpha}\boldsymbol{k}$, where a dot denotes time derivative.

We shall throughout the paper consider the problem in the relative frame of reference. The incoming waves described in this frame of reference are determined by the potential

$$\Phi^I = \mathrm{Re}[(\mathrm{i}Ag/\omega)\phi^I \mathrm{e}^{\mathrm{i}\omega t}], \qquad \phi^I = Ch(kz)\mathrm{e}^{-\mathrm{i}kR\cos(\beta-\theta)}, \tag{2.1}$$

where $Ch(kz) \equiv \cosh k(z+h)/\cosh kh$, and A, k and ω denote the amplitude, wavenumber and frequency, respectively, of the incoming waves, h the water depth, and g the acceleration due to gravity; ω and k obey the dispersion relation

$$K = k\tanh kh, \quad \text{where} \quad K = \omega^2/g. \tag{2.2}$$

The wave angle β is defined as the angle between the positive x-axis and the wave direction. In (2.1) we have also introduced polar coordinates by $x = R\cos\theta$, $y = R\sin\theta$.

The slow rotation of the body introduces effectively a slowly varying wave angle to

an observer in the relative frame of reference. This is determined by $\beta(t) + \alpha(t) = \beta_0$, which means that $\mathrm{d}\beta/\mathrm{d}t = -\Omega$. β_0 is the wave angle in the fixed frame of reference. We let the rotation angle α be arbitrary and the non-dimensional wavenumber kl be of order one, where l denotes the characteristic length of the body. We assume, however, that Ω is small compared to the wave frequency. This is a relevant assumption, since the resonance frequency in the horizontal modes of motion of a lightly moored floating body most often is much smaller than the wave frequency. Introducing the small parameter $\epsilon = \Omega/\omega$ we shall in the mathematical analysis apply perturbation expansions in A/l and ϵ, retaining terms up to order $(A/l)^2$ and ϵ. (This means e.g. that terms proportional to $\dot{\Omega}/\omega^2 = O(\epsilon^2)$ are neglected.) The perturbed problem then has two timescales, a fast timescale with characteristic time $1/\omega$ and a slow timescale with characteristic time $1/\Omega$. To obtain the wave-drift damping, a time-average over the fast timescale is applied.

Let $\boldsymbol{v}$ denote the fluid velocity in the relative frame of reference. This may be decomposed as $\boldsymbol{v} = \nabla\Phi' - \Omega\boldsymbol{k} \times \boldsymbol{x}$, where Φ' is a velocity potential and $-\Omega\boldsymbol{k} \times \boldsymbol{x}$ denotes the velocity introduced to an observer moving from the fixed to the relative frame of reference. The potential Φ' satisfies the Laplace equation since $\nabla \cdot \boldsymbol{v} = 0$, according to the assumptions. We decompose Φ' as

$$\Phi' = \Omega\chi_6 + \Phi + \psi^{(2)}, \tag{2.3}$$

where $\Omega\chi_6$ denotes the potential due to the flow generated by the body when there are no waves, Φ the linear wave potential which is proportional to the wave amplitude and is due to the incoming, scattered and radiated waves, and $\psi^{(2)}$ the time-averaged potential which is proportional to the wave amplitude squared. It is convenient to introduce

$$\boldsymbol{w} = -\boldsymbol{k} \times \boldsymbol{x} + \nabla\chi_6, \tag{2.4}$$

where $\boldsymbol{w}$ satisfies the rigid wall condition at the body, at the free surface and at the sea floor. Furthermore, $\nabla\chi_6$ vanishes for $R \to \infty$.

3. The boundary conditions for Φ

3.1. *The free-surface boundary condition*

The free-surface boundary condition for Φ is obtained by applying the individual derivative to the Bernoulli equation for the pressure at the free surface. After linearizing with respect to the wave amplitude, we find (see GP, § 3)

$$\frac{\partial^2\Phi}{\partial t^2} + 2\Omega\boldsymbol{w} \cdot \nabla_h \frac{\partial\Phi}{\partial t} + \Omega\frac{\partial\Phi}{\partial t}\nabla_h \cdot \boldsymbol{w} + g\frac{\partial\Phi}{\partial z} = 0 \quad \text{at} \quad z = 0, \tag{3.1}$$

where ∇_h denotes the horizontal gradient. We next introduce the decomposition of Φ as follows:

$$\Phi = \mathrm{Re}\left\{ \frac{\mathrm{i}Ag}{\omega}\phi_D \mathrm{e}^{\mathrm{i}\omega t} + \sum_{j=1}^{6} \frac{\mathrm{d}}{\mathrm{d}t}\left(\xi_j \mathrm{e}^{\mathrm{i}\omega t}\right)\phi_j \right\}, \tag{3.2}$$

where the first part represents the incoming and scattered waves, and the second part the radiation potentials. ξ_j are the linear responses, see (3.14).

We here consider the radiation potentials. The corresponding diffraction potential and its decomposition were described by GP; a short account is given in Appendix A. As already noted, the motion in the relative frame of reference depends on the

slowly varying wave angle $\beta(t)$. To first order in ϵ we then have

$$\frac{\mathrm{d}}{\mathrm{d}t}(\xi_j \mathrm{e}^{\mathrm{i}\omega t}) = \left(\mathrm{i}\omega\xi_j + \frac{\mathrm{d}\xi_j}{\mathrm{d}t}\right)\mathrm{e}^{\mathrm{i}\omega t} = \mathrm{i}\omega\left(\xi_j + \mathrm{i}\epsilon\frac{\partial\xi_j}{\partial\beta}\right)\mathrm{e}^{\mathrm{i}\omega t}, \quad j = 1,\ldots,6 \tag{3.3}$$

where we have used $\mathrm{d}\beta/\mathrm{d}t = -\Omega$. We may show that $\partial\phi_j/\partial t = O(\epsilon^2)$ for $j = 1,\ldots,6$, see the comments on the last two lines of § 3.2. Inserting (3.2)–(3.3) into (3.1) and retaining terms up to first order in ϵ, we obtain

$$-K\left(\xi_j + 3\mathrm{i}\epsilon\frac{\partial\xi_j}{\partial\beta}\right)\phi_j + \mathrm{i}\epsilon K\xi_j(2\boldsymbol{w}\cdot\nabla_h\phi_j + \phi_j\nabla_h\cdot\boldsymbol{w}) + \left(\xi_j + \mathrm{i}\epsilon\frac{\partial\xi_j}{\partial\beta}\right)\frac{\partial\phi_j}{\partial z} = 0 \tag{3.4}$$

at $z = 0$, where the sum over j is understood. It is now convenient to introduce perturbation expansions for ξ_j and $\xi_j\phi_j$. The boundary condition (3.4) suggests expansions as follows:

$$\xi_j = \xi_j^0 + \epsilon\xi_j^1, \quad j = 1,\ldots,6, \tag{3.5}$$

$$\xi_j\phi_j = \xi_j^0\phi_j^0 + \epsilon\left(\xi_j^1\phi_j^0 + (\partial\xi_j^0/\partial\beta)\phi_j^{11} + \xi_j^0\psi_j^1\right), \tag{3.6}$$

where the potentials ϕ_j^{11} and ψ_j^1 are specified below. To order ϵ^0 we obtain

$$-K\phi_j^0 + \frac{\partial\phi_j^0}{\partial z} = 0 \quad \text{at} \quad z = 0. \tag{3.7}$$

To order ϵ^1 we find

$$-K\left\{\left(\xi_j^1\phi_j^0 + \xi_j^0\psi_j^1 + \frac{\partial\xi_j^0}{\partial\beta}\left(\phi_j^{11} + 3i\phi_j^0\right)\right)\right\} + \mathrm{i}K\xi_j^0(2\boldsymbol{w}\cdot\nabla_h\phi_j^0 + \phi_j^0\nabla_h\cdot\boldsymbol{w})$$
$$+\left\{\xi_j^1\frac{\partial\phi_j^0}{\partial z} + \xi_j^0\frac{\partial\psi_j^1}{\partial z} + \frac{\partial\xi_j^0}{\partial\beta}\left(\frac{\partial\phi_j^{11}}{\partial z} + \mathrm{i}\frac{\partial\phi_j^0}{\partial z}\right)\right\} = 0 \quad \text{at} \quad z = 0. \tag{3.8}$$

Exploiting (3.7), this gives

$$-K\phi_j^{11} + \frac{\partial\phi_j^{11}}{\partial z} = 2iK\phi_j^0 \quad \text{at} \quad z = 0, \tag{3.9}$$

$$-K\psi_j^1 + \frac{\partial\psi_j^1}{\partial z} = 2\mathrm{i}K\frac{\partial\phi_j^0}{\partial\theta} - 2\mathrm{i}K\nabla_h\phi_j^0\cdot\nabla\chi_6 - \mathrm{i}K\phi_j^0\nabla_h^2\chi_6 \quad \text{at} \quad z = 0 \tag{3.10}$$

for $j = 1,\ldots,6$. In the far-field analysis carried out later, among other things to obtain the wave-drift damping coefficients, it is convenient to decompose ψ_j^1 into $\psi_j^1 = \phi_j^{12} + \phi_j^{13}$, where ϕ_j^{12} and ϕ_j^{13} at the free surface satisfy

$$-K\phi_j^{12} + \frac{\partial\phi_j^{12}}{\partial z} = 2\mathrm{i}K\frac{\partial\phi_j^0}{\partial\theta} \quad \text{at} \quad z = 0, \tag{3.11}$$

$$-K\phi_j^{13} + \frac{\partial\phi_j^{13}}{\partial z} = -2\mathrm{i}K\nabla_h\phi_j^0\cdot\nabla\chi_6 - \mathrm{i}K\phi_j^0\nabla_h^2\chi_6 \quad \text{at} \quad z = 0 \tag{3.12}$$

for $j = 1,\ldots,6$. The potentials ϕ_j^{11} and ϕ_j^{12} may be expressed in terms of ϕ_j^0 by

$$\phi_j^{11} = 2\mathrm{i}K\frac{\partial\phi_j^0}{\partial K}, \qquad \phi_j^{12} = 2\mathrm{i}K\frac{\partial^2\phi_j^0}{\partial K\,\partial\theta}. \tag{3.13}$$

3.2. *The boundary condition at the body*

We next consider the kinematic boundary condition at the surface of the body. The linear body motions are determined by

$$\tilde{\boldsymbol{B}} = \tilde{\boldsymbol{\xi}} + \tilde{\boldsymbol{\alpha}} \times \boldsymbol{x}, \tag{3.14}$$

where $\tilde{\boldsymbol{\xi}} = \mathrm{Re}\{(\xi_1, \xi_2, \xi_3)\mathrm{e}^{\mathrm{i}\omega t}\}$ and $\tilde{\boldsymbol{\alpha}} = \mathrm{Re}\{(\xi_4, \xi_5, \xi_6)\mathrm{e}^{\mathrm{i}\omega t}\}$ denote respectively the first-order translations and rotations. We note that frequencies of the body oscillations in general differ from ω when $\Omega \neq 0$, see § 6.3. The kinematic boundary condition gives

$$\boldsymbol{N} \cdot \{\Omega \boldsymbol{w} + \nabla \Phi + \nabla \psi^{(2)}\} = \boldsymbol{N} \cdot \mathrm{d}\tilde{\boldsymbol{B}}/\mathrm{d}t, \tag{3.15}$$

which applies at the instantaneous position of the body, and where $\boldsymbol{N}$ denotes the instantaneous unit normal vector, pointing out of the fluid. We then expand (3.15) about the mean position of the body, which we denote by S_B. The normal vector $\boldsymbol{N}$ may be expressed by $\boldsymbol{N} = \boldsymbol{n} + \tilde{\boldsymbol{\alpha}} \times \boldsymbol{n}$, where $\boldsymbol{n} = (n_1, n_2, n_3)$ denotes the unit normal vector when $\tilde{\boldsymbol{\alpha}} = 0$. After expanding the term in curly brackets in (3.15) we find

$$(\boldsymbol{n} + \tilde{\boldsymbol{\alpha}} \times \boldsymbol{n}) \cdot \{\Omega \boldsymbol{w} + \nabla \Phi + \nabla \psi^{(2)} + \tilde{\boldsymbol{B}} \cdot \nabla(\Omega \boldsymbol{w} + \nabla \Phi)\} = (\boldsymbol{n} + \tilde{\boldsymbol{\alpha}} \times \boldsymbol{n}) \cdot \mathrm{d}\tilde{\boldsymbol{B}}/\mathrm{d}t \tag{3.16}$$

where terms proportional to $O(A^3, \epsilon A^2, \epsilon^2)$ are omitted. For the terms in (3.16) proportional to $\mathrm{e}^{\mathrm{i}\omega t}$ we find

$$\boldsymbol{n} \cdot \nabla \Phi + \Omega[(\tilde{\boldsymbol{\alpha}} \times \boldsymbol{n}) \cdot \boldsymbol{w} + \boldsymbol{n} \cdot (\tilde{\boldsymbol{B}} \cdot \nabla \boldsymbol{w})] = \boldsymbol{n} \cdot \mathrm{d}\tilde{\boldsymbol{B}}/\mathrm{d}t. \tag{3.17}$$

We then utilize the vector relation

$$\boldsymbol{n} \cdot (\tilde{\boldsymbol{B}} \cdot \nabla \boldsymbol{w}) = (\tilde{\boldsymbol{B}} \times \boldsymbol{n}) \cdot (\nabla \times \boldsymbol{w}) + \tilde{\boldsymbol{B}} \cdot \partial \boldsymbol{w}/\partial n \tag{3.18}$$

and

$$\tilde{\boldsymbol{B}} \cdot \frac{\partial \boldsymbol{w}}{\partial n} = \tilde{\boldsymbol{\xi}} \cdot \frac{\partial \boldsymbol{w}}{\partial n} + \tilde{\boldsymbol{\alpha}} \cdot \frac{\partial}{\partial n}(\boldsymbol{x} \times \boldsymbol{w}) - (\tilde{\boldsymbol{\alpha}} \times \boldsymbol{n}) \cdot \boldsymbol{w}. \tag{3.19}$$

In our case, $\boldsymbol{w}$ has non-zero vorticity, given by

$$\nabla \times \boldsymbol{w} = -2\boldsymbol{k}. \tag{3.20}$$

Combining (3.17)–(3.20) we find

$$\boldsymbol{n} \cdot \nabla \Phi = \boldsymbol{n} \cdot \frac{\mathrm{d}}{\mathrm{d}t}(\tilde{\boldsymbol{\xi}} + \tilde{\boldsymbol{\alpha}} \times \boldsymbol{x}) - \Omega \left\{ \tilde{\boldsymbol{\xi}} \cdot \left(\frac{\partial \boldsymbol{w}}{\partial n} + 2\boldsymbol{k} \times \boldsymbol{n} \right) + \tilde{\boldsymbol{\alpha}} \cdot \left[\frac{\partial}{\partial n}(\boldsymbol{x} \times \boldsymbol{w}) + 2\boldsymbol{x} \times (\boldsymbol{k} \times \boldsymbol{n}) \right] \right\}. \tag{3.21}$$

We then insert (3.2), (3.3), (3.5) and (3.6) into (3.21) and obtain

$$\frac{\partial \phi_j^0}{\partial n} = n_j, \quad j = 1, \ldots, 6 \quad \text{at } S_B \tag{3.22}$$

where $(n_4, n_5, n_6) = \boldsymbol{x} \times \boldsymbol{n}$, and

$$\frac{\partial \phi_j^{11}}{\partial n} = 0, \quad j = 1, \ldots, 6 \quad \text{at } S_B, \tag{3.23}$$

$$\frac{\partial \psi_j^1}{\partial n} = -im_j, \quad j = 1, \ldots, 6 \quad \text{at } S_B. \tag{3.24}$$

Here, generalized m_j-terms are determined by

$$(m_1, m_2, m_3) = -\frac{\partial \boldsymbol{w}}{\partial n} - 2\boldsymbol{k} \times \boldsymbol{n}, \tag{3.25}$$

$$(m_4, m_5, m_6) = -\frac{\partial}{\partial n}(\boldsymbol{x} \times \boldsymbol{w}) - 2\boldsymbol{x} \times (\boldsymbol{k} \times \boldsymbol{n}). \tag{3.26}$$

Thus, in the present problem m_j contain the extra terms $-2\boldsymbol{k}\times\boldsymbol{n}$ and $-2\boldsymbol{x}\times(\boldsymbol{k}\times\boldsymbol{n})$ due to the rotation of the body. These terms are absent for bodies performing small oscillations superposed on a translatory motion.

We note that the boundary conditions for ϕ_j^0, ϕ_j^{11} and ψ_j^1 do not depend on the wave angle β, which means that these potentials do not depend on β.

3.3. *The potentials in the far field*

The potential $\Phi-\Phi^I$ is generated by the presence of the floating body, and represents outgoing waves at some distance from the body. The far-field forms of the potentials ϕ_j^0 and ϕ_j^{13} become

$$\phi_j^0 = R^{-1/2}H_j^0(\theta)Ch(kz)\mathrm{e}^{-\mathrm{i}kR}(1+O((kR)^{-1})), \qquad j=1,\ldots,6, \tag{3.27}$$

$$\phi_j^{13} = R^{-1/2}H_j^{13}(\theta)Ch(kz)\mathrm{e}^{-\mathrm{i}kR}(1+O((kR)^{-1})), \qquad j=1,\ldots,6, \tag{3.28}$$

where H_j^0 and H_j^{13} are determined below by (5.15) and (5.16), respectively. For ϕ_j^{11} and ψ_j^1 we may, using (3.27) and (3.28), show that

$$\frac{\partial\phi_j^{11}}{\partial R} = -\mathrm{i}k\phi_j^{11} + K\frac{\partial k}{\partial K}\phi_j^0(1+O((kR)^{-1})), \qquad j=1,\ldots,6, \tag{3.29}$$

$$\frac{\partial\psi_j^1}{\partial R} = -\mathrm{i}k\psi_j^1 + K\frac{\partial k}{\partial K}\frac{\partial\phi_j^0}{\partial\theta}(1+O((kR)^{-1})), \qquad j=1,\ldots,6. \tag{3.30}$$

Similar relations may be derived for the various components of the diffraction potential ϕ_D^1, see Appendix A. We may for finite value of R apply (3.29) and (3.30) in the far-field analysis, since all terms of the expansions of the potentials in principle are included. In deriving integral equations for the potentials and formulae for the forces and moments, we shall integrate the potentials at a control surface for large, but finite R. We remark that the terms proportional to $R^{1/2}\mathrm{e}^{-\mathrm{i}kR}$ in ϕ_j^{11}, ψ_j^1 (and ϕ_D^1) always disappear in these formulae, which means that we may let $R\to\infty$ to obtain the final results.

3.4. *The boundary condition at the sea floor*

At the sea floor all the potentials satisfy the rigid wall condition, i.e.

$$\frac{\partial}{\partial n}(\text{potential}) = 0 \quad \text{at} \quad z=-h. \tag{3.31}$$

4. The potential $\psi^{(2)}$

The second-order potential $\psi^{(2)}$ always appears in the formulae for the time-averaged pressure, force and moment multiplied by Ω, and it suffices to consider the boundary value problem for $\psi^{(2)}$ when $\Omega=0$, to leading order. The free-surface boundary condition for $\psi^{(2)}$ then reads

$$\frac{\partial\psi^{(2)}}{\partial z} = -\frac{gA^2}{2\omega}\mathrm{Im}\left(\phi^0\frac{\partial^2\phi^{0*}}{\partial z^2}\right) \quad \text{at} \quad z=0 \tag{4.1}$$

where an asterisk denotes complex conjugate. The boundary condition at S_B is obtained from the time-averaged part of (3.16), giving

$$\frac{\partial\psi^{(2)}}{\partial n} = \frac{gA^2}{2\omega}\mathrm{Im}\{\boldsymbol{B}^0\cdot(\boldsymbol{n}\cdot\nabla)\nabla\phi^{0*} - \boldsymbol{C}^0\cdot(K\boldsymbol{B}^{0*}-\nabla\phi^{0*})\} \quad \text{at } S_B \tag{4.2}$$

where $\boldsymbol{B}^0 = [(\xi_1^0, \xi_2^0, \xi_3^0) + (\xi_4^0, \xi_5^0, \xi_6^0) \times \boldsymbol{x}]/A$, $\boldsymbol{C}^0 = (\xi_4^0, \xi_5^0, \xi_6^0) \times \boldsymbol{n}/A$. A complete discussion of how to obtain $\psi^{(2)}$ is given in Grue & Palm (1993) (for $h = \infty$).

The theory is intended for application to sea states with several spectral components, as mentioned in the Introduction. Under the assumption of a low resonance frequency of the oscillating system, or if the wave spectrum is narrow-banded, the important difference frequency components of the forces and potentials are due to neighbouring frequencies. For ω_j and ω_k similar we find that the boundary conditions at the free surface lead to

$$\begin{aligned}\frac{\partial \psi^{(2)}}{\partial z}(\omega_j, \omega_k) &= \frac{\partial \psi^{(2)}}{\partial z}(\omega_j, \omega_j)[1 + O((\omega_j - \omega_k)/\omega_j)] \\ &= \frac{\partial \psi^{(2)}}{\partial z}(\omega_j, \omega_j)[1 + O(\epsilon)] \quad \text{at} \quad z = 0.\end{aligned}$$

A similar result is true for $\partial\psi^{(2)}/\partial n$. This means that (4.1)–(4.2) determine the leading terms of the boundary conditions at S_F and S_B for $\psi^{(2)}$ in the spectral case for two neighbouring frequencies ω_j and ω_k.

5. Integral equations

5.1. *The potentials ϕ_j^0 and their derivatives*

To solve the boundary value problems for ϕ_j^0 we first introduce a Green function, $G^0(x', y', z', x, y, z)$, being a sink at $\boldsymbol{x} = \boldsymbol{x}' = (x', y', z')$, satisfying the free-surface boundary condition (3.7). This Green function may be found in e.g. Wehausen & Laitone (1960, equation 13.18). By applying Green's theorem to ϕ_j^0 and G^0 it may be shown that in the radiation problem ϕ_j^0 satisfies

$$\int_{S_B} \left(\phi_j^0 \frac{\partial G^0}{\partial n} - G^0 n_j \right) \mathrm{d}S = \begin{cases} -2\pi\phi_j^0(\boldsymbol{x}), & \boldsymbol{x} \in S_B, \\ -4\pi\phi_j^0(\boldsymbol{x}), & \boldsymbol{x} \in \mathscr{V}, \end{cases} \quad j = 1, \ldots, 6. \tag{5.1}$$

Here, $\mathscr{V}$ denotes the fluid volume enclosed by the mean body surface, S_B, the mean free surface, S_F, and the vertical circular cylinder, S_R, with finite radius R. The first case is an integral equation for ϕ_j^0.

The various derivatives of the potentials ϕ_j^0 may be obtained by means of integral equations. By differentiating (5.1) with respect to K, we obtain that $\partial\phi_j^0/\partial K$ is determined by

$$\int_{S_B} \left(\phi_{j,K}^0 \frac{\partial G^0}{\partial n} + \phi_j^0 \frac{\partial^2 G^0}{\partial n \, \partial K} - \frac{\partial G^0}{\partial K} n_j \right) \mathrm{d}S = \begin{cases} -2\pi\phi_{j,K}^0(\boldsymbol{x}), & \boldsymbol{x} \in S_B, \\ -4\pi\phi_{j,K}^0(\boldsymbol{x}), & \boldsymbol{x} \in \mathscr{V}, \end{cases} \quad j = 1, \ldots, 6 \tag{5.2}$$

where $\phi_{j,K}^0 \equiv \partial\phi_j^0/\partial K$. Multiplying $\phi_{j,K}^0$ by $2\mathrm{i}K$ we obtain ϕ_j^{11} $(j = 1, \ldots, 6)$.

The potential $\partial^2\phi_j^0/\partial\theta\partial K$ is determined by differentiating (5.2) with respect to the θ-variable, i.e.

$$\int_{S_B} \left(\phi_{j,K}^0 \frac{\partial^2 G^0}{\partial\theta\partial n} + \phi_j^0 \frac{\partial^3 G^0}{\partial K \, \partial\theta\partial n} - \frac{\partial^2 G^0}{\partial K \, \partial\theta} n_j \right) \mathrm{d}S = -4\pi\phi_{j,\theta K}^0(\boldsymbol{x}), \quad \boldsymbol{x} \in \mathscr{V}, \quad j = 1, \ldots, 6 \tag{5.3}$$

which, multiplied by $2\mathrm{i}K$, determines ϕ_j^{12} for $\boldsymbol{x} \in \mathscr{V}$.

5.2. *The potential ψ_j^1*

Owing to the boundary condition (3.24) at S_B, it is more convenient to derive an integral equation for the sum $\psi_j^1 = \phi_j^{12} + \phi_j^{13}$ at S_B than for the potential ϕ_j^{13}. We

then first apply Green's theorem to ψ_j^1 and G^0, giving

$$\int_{S_B}\left(\psi_j^1\frac{\partial G^0}{\partial n}-G^0\frac{\partial\psi_j^1}{\partial n}\right)\mathrm{d}S+\int_{S_F+S_R}\left(\psi_j^1\frac{\partial G^0}{\partial n}-G^0\frac{\partial\psi_j^1}{\partial n}\right)\mathrm{d}S=\begin{cases}-2\pi\psi_j^1(\boldsymbol{x}), & \boldsymbol{x}\in S_B,\\ -4\pi\psi_j^1(\boldsymbol{x}), & \boldsymbol{x}\in\mathscr{V}.\end{cases}\tag{5.4}$$

By applying the free-surface boundary conditions for ψ_j^1 and G^0 (see (3.10) and (3.7), respectively), (5.4) reduces to

$$\int_{S_B}\left(\psi_j^1\frac{\partial G^0}{\partial n}-G^0\frac{\partial\psi_j^1}{\partial n}\right)\mathrm{d}S+2\mathrm{i}K\int_{S_F}G^0\left(-\frac{\partial\phi_j^0}{\partial\tilde{\theta}}+\nabla_h\phi_j^0\cdot\nabla_h\chi_6+\tfrac{1}{2}\phi_j^0\nabla_h^2\chi_6\right)\mathrm{d}S$$
$$+\int_{S_R}\left(\psi_j^1\frac{\partial G^0}{\partial n}-G^0\frac{\partial\psi_j^1}{\partial n}\right)\mathrm{d}S=\begin{cases}-2\pi\psi_j^1(\boldsymbol{x}), & \boldsymbol{x}\in S_B,\\ -4\pi\psi_j^1(\boldsymbol{x}), & \boldsymbol{x}\in\mathscr{V}.\end{cases}\tag{5.5}$$

Following GP, we introduce an auxiliary function $G^1=2\mathrm{i}K\partial^2G^0/\partial\tilde{\theta}\partial K$, where $\tilde{\theta}$ is defined by $x'=\tilde{R}\cos\tilde{\theta}$, $y'=\tilde{R}\sin\tilde{\theta}$, $\tilde{R}^2=x'^2+y'^2$. Applying Green's theorem to ϕ_j^0 and G^1, and introducing the boundary conditions for ϕ_j^0 and G^0 at the free surface, we obtain

$$\int_{S_B}\left(\phi_j^0\frac{\partial G^1}{\partial n}-G^1\frac{\partial\phi_j^0}{\partial n}\right)\mathrm{d}S+2\mathrm{i}K\int_{S_F}\phi_j^0\frac{\partial G^0}{\partial\tilde{\theta}}\mathrm{d}S+\int_{S_R}\left(\phi_j^0\frac{\partial G^1}{\partial n}-G^1\frac{\partial\phi_j^0}{\partial n}\right)\mathrm{d}S=0.\tag{5.6}$$

Subtracting (5.6) from (5.5) gives

$$\int_{S_B}\left(\psi_j^1\frac{\partial G^0}{\partial n}-G^0\frac{\partial\psi_j^1}{\partial n}-\phi_j^0\frac{\partial G^1}{\partial n}+G^1\frac{\partial\phi_j^0}{\partial n}\right)\mathrm{d}S$$
$$+2\mathrm{i}K\int_{S_F}\left(-\frac{\partial}{\partial\tilde{\theta}}(G^0\phi_j^0)+G^0(\nabla_h\phi_j^0\cdot\nabla_h\chi_6+\tfrac{1}{2}\phi_j^0\nabla_h^2\chi_6)\right)\mathrm{d}S$$
$$+\int_{S_R}\left(\psi_j^1\frac{\partial G^0}{\partial n}-G^0\frac{\partial\psi_j^1}{\partial n}-\phi_j^0\frac{\partial G^1}{\partial n}+G^1\frac{\partial\phi_j^0}{\partial n}\right)\mathrm{d}S=\begin{cases}-2\pi\psi_j^1(\boldsymbol{x}), & \boldsymbol{x}\in S_B,\\ -4\pi\psi_j^1(\boldsymbol{x}), & \boldsymbol{x}\in\mathscr{V}.\end{cases}\tag{5.7}$$

We note that ψ_j^1 and G^1 satisfy the same condition at S_R, see (3.30). By applying this condition together with the far-field condition (3.27) for ϕ_j^0 and G^0, and then partially integrating with respect to the $\tilde{\theta}$-variable, we find that the integral over S_R vanishes for $R\to\infty$. The integral over S_F in (5.7) may be further developed, and after some algebra we find for this integral

$$-\int_{S_F}\phi_j^0L_h(G^0,\chi_6)\mathrm{d}S,\tag{5.8}$$

where

$$L_h(G^0,\chi_6)=2\mathrm{i}K\nabla_hG^0\cdot\nabla_h\chi_6+\mathrm{i}KG^0\nabla_h^2\chi_6.\tag{5.9}$$

We then apply the boundary conditions for ϕ_j^0 and ψ_j^1 at S_B, (3.22) and (3.24), respectively. The latter boundary condition leads to integrals over the m_j-terms which require evaluation of the derivative of $\boldsymbol{w}$ along the normal of S_B, and are not of suitable form. However, by using a variant of Stokes theorem, and applying the

properties of $\boldsymbol{w}$, where $\nabla \times \boldsymbol{w}$ is non-zero, we may rewrite these integrals as

$$\int_{S_B} G^0 m_j \mathrm{d}S = -\int_{S_B} \boldsymbol{w} \cdot \nabla G^0 n_j \mathrm{d}S. \tag{5.10}$$

In (5.10) we have also assumed that the body is wall-sided at the water line. Thus, (5.7) becomes

$$\int_{S_B} \left(\psi_j^1 \frac{\partial G^0}{\partial n} - \mathrm{i}\boldsymbol{w} \cdot \nabla G^0 n_j - \phi_j^0 \frac{\partial G^1}{\partial n} + G^1 n_j \right) \mathrm{d}S$$
$$- \int_{S_F} \phi_j^0 L_h(G^0, \chi_6) \mathrm{d}S = \begin{cases} -2\pi\psi_j^1(\boldsymbol{x}), & \boldsymbol{x} \in S_B, \\ -4\pi\psi_j^1(\boldsymbol{x}), & \boldsymbol{x} \in \mathscr{V}, \end{cases} \tag{5.11}$$

for $j = 1, \ldots, 6$, where the first case is an integral equation for ψ_j^1.

The integral equations for the various potentials are solved by means of a low-order panel method, where the geometry is discretized by means of quadrilaterals. The most important numerical aspects of the method are commented on in Appendix B.

Integral equations for the potentials $\partial\phi_D^0/\partial\beta$, $\partial^2\phi_D^0/\partial\beta\partial K$ and $\phi_7^{12} + \phi_7^{13}$ in the diffraction problem were derived in GP, § 4.

5.3. *Far-field amplitudes*

We are now able to determine the far-field amplitudes of the potentials ϕ_j^0 and ϕ_j^{13}, see (3.27)–(3.28). First we note that the far-field form of G^0 reads

$$G^0 = R^{-1/2} h^0(\theta, \boldsymbol{x}') Ch(kz) \mathrm{e}^{-\mathrm{i}kR} (1 + O((kR^{-1}))) \tag{5.12}$$

where

$$h^0 = \frac{(2\pi k)^{1/2}}{C_g(kh)} (\tanh kh + 1) \left(\mathrm{e}^{kz'} + \mathrm{e}^{-k(z'+2h)} \right) \mathrm{e}^{k(\mathrm{i}x' \cos\theta + iy' \sin\theta) - \mathrm{i}\pi/4} \tag{5.13}$$

and

$$C_g(kh) = \tanh kh + \frac{kh}{\cosh^2 kh} \equiv \frac{\partial\omega/\partial k}{g/2\omega}. \tag{5.14}$$

(C_g denotes the ratio between the group velocity of a wave with frequency ω at finite and infinite water depth, respectively.) The far-field amplitude H_j^0 is obtained by inserting the far-field form of G^0 into (5.1), i.e.

$$4\pi H_j^0(\theta) = -\int_{S_B} \left(\phi_j^0 \frac{\partial h^0}{\partial n} - h^0 n_j \right) \mathrm{d}S. \tag{5.15}$$

The far-field amplitude H_j^{13} is obtained by first subtracting (5.3) multiplied by $2\mathrm{i}K$ from (5.11) and then using (5.12), giving

$$4\pi H_j^{13}(\theta) = -\int_{S_B} \left(\psi_j^1 \frac{\partial h^0}{\partial n} - 2\mathrm{i}K\phi_{j,K}^0 \frac{\partial^2 h^0}{\partial\theta\partial n} - \mathrm{i}\nabla h^0 \cdot \boldsymbol{w} n_j \right) \mathrm{d}S + \int_{S_F} \phi_j^0 L_h(h^0, \chi_6) \mathrm{d}S. \tag{5.16}$$

6. First-order forces and body responses

6.1. *Exciting forces and generalized Haskind relations*

An expression for the pressure in a rotating frame of reference was derived by GP, equation (2.7). From this we find that the linear dynamic pressure reads $p = -\rho(\partial\Phi/\partial t + \Omega \boldsymbol{w} \cdot \nabla\Phi)$, where ρ denotes the density of the fluid. The linear exciting

forces and moments are obtained by integrating the pressure over the body surface. By setting $\xi_j = 0$ $(j = 1, \ldots, 6)$ in Φ we obtain

$$F_i^{ex} = -\rho \int_{S_B} \left(\frac{\partial \Phi}{\partial t} + \Omega \boldsymbol{w} \cdot \nabla \Phi \right) n_i \mathrm{d}S$$
$$= \rho g A \mathrm{Re} \left\{ \mathrm{e}^{\mathrm{i}\omega t} \left(\int_{S_B} \phi_D^0 n_i \mathrm{d}S + \epsilon \int_{S_B} \left(\mathrm{i} \frac{\partial \phi_D^0}{\partial \beta} + \phi_D^1 - \boldsymbol{w} \cdot \nabla \phi_D^0 \right) n_i \mathrm{d}S \right) \right\}, \quad i = 1, \ldots, 6. \tag{6.1}$$

Introducing

$$X_i^0 = \rho g \int_{S_B} \phi_D^0 n_i \mathrm{d}S, \qquad X_i^1 = \rho g \int_{S_B} (\phi_D^1 - \mathrm{i}\boldsymbol{w} \cdot \nabla \phi_D^0) n_i \mathrm{d}S \tag{6.2}$$

we may write

$$F_i^{ex} = A \, \mathrm{Re} \left\{ \left(X_i^0 + \epsilon \left(\mathrm{i} \frac{\partial X_i^0}{\partial \beta} + X_i^1 \right) \right) \mathrm{e}^{\mathrm{i}\omega t} \right\}. \tag{6.3}$$

The exciting forces may, when $\Omega = 0$, be found from the Haskind relations, which in one form expresses X_i^0 in terms of the far-field amplitude of ϕ_i^0 (see e.g. Newman 1977 § 6.18),

$$\frac{X_i^0}{\rho g} = \int_{S_B} \phi_D^0 n_i \mathrm{d}S = -\int_{S_R} (\phi^I \phi_{i,n}^0 - \phi_i^0 \phi_{,n}^I) \mathrm{d}S$$
$$= \left(\frac{2\pi}{k} \right)^{1/2} C_g(kh) H_i^0(\beta + \pi) \mathrm{e}^{\mathrm{i}\pi/4}, \quad i = 1, \ldots, 6, \tag{6.4}$$

where $C_g(kh)$ is given by (5.14) and H_i^0 by (5.15). We now proceed to derive similar relations for X_i^1. By using the variant of Stokes theorem (5.10) and the body boundary conditions for ϕ_i^0 and ψ_i^1, see (3.22) and (3.24), we find that X_i^1 may be written

$$\frac{X_i^1}{\rho g} = \int_{S_B} (\phi_D^1 \phi_{i,n}^0 - \phi_D^0 \psi_{i,n}^1) \mathrm{d}S = \int_{S_B} (\psi_7^1 \phi_{i,n}^0 - \phi_D^0 \psi_{i,n}^1) \mathrm{d}S + \int_{S_B} \phi_7^{11} \phi_{i,n}^0 \mathrm{d}S \tag{6.5}$$

where we have introduced $\psi_7^1 = \phi_7^{12} + \phi_7^{13}$, such that $\phi_D^1 = \phi_7^{11} + \psi_7^1$ (see also Appendix A). Furthermore, $(\ )_{,n}$ denotes $\partial/\partial n$. We may add to (6.5) the integral $\int_{S_B} (-\phi_i^0 \psi_{7,n}^1 + \psi_i^1 \phi_{D,n}^0) \mathrm{d}S$, which equals zero, since $\psi_{7,n}^1 = \phi_{D,n}^0 = 0$ at S_B. By applying Green's theorem and the body boundary conditions for the potentials involved, the first integral on the right of (6.5) is converted to integrals over S_F and S_R, i.e.

$$\frac{X_i^1}{\rho g} = -\int_{S_F + S_R} (\psi_7^1 \phi_{i,n}^0 - \phi_i^0 \psi_{7,n}^1 + \psi_i^1 \phi_{D,n}^0 - \phi_D^0 \psi_{i,n}^1) \mathrm{d}S + \int_{S_B} \phi_7^{11} \phi_{i,n}^0 \mathrm{d}S. \tag{6.6}$$

Since $\psi_i^1 = \phi_i^{12} + \phi_i^{13}$ $(i = 1, \ldots, 7)$, the integral over S_R in (6.6) may be written as $I_X^2 + I_X^3$, where

$$I_X^j = -\int_{S_R} (\phi_7^{1j} \phi_{i,n}^0 - \phi_i^0 \phi_{7,n}^{1j} + \phi_i^{1j} \phi_{D,n}^0 - \phi_D^0 \phi_{i,n}^{1j}) \mathrm{d}S, \qquad j = 2, 3. \tag{6.7}$$

We may show, by applying the far-field forms of ϕ_i^0 and ϕ_i^{13}, that I_X^3 becomes

$$I_X^3 = \int_{S_R} (\phi^I \phi_{i,n}^{13} - \phi_i^{13} \phi_{,n}^I) \mathrm{d}S. \tag{6.8}$$

Next we consider I_X^2. Exploiting that $\phi_7^{12} = 2\mathrm{i}K\partial^2\phi_D^0/\partial K\partial\theta$, $\phi_i^{12} = 2\mathrm{i}K\partial^2\phi_i^0/\partial K\partial\theta$, and applying partial integration with respect to the θ-variable, we find

$$I_X^2 = -2\mathrm{i}K\frac{\partial}{\partial K}\int_{S_R}(\phi_{D,\theta}^0\phi_{i,n}^0 - \phi_i^0\phi_{D,n\theta}^0)\mathrm{d}S. \tag{6.9}$$

We may then show, by applying the far-field form of ϕ_i^0 $(i = 1,\ldots,7)$ that the contribution from $\phi_{7,\theta}^0\phi_{i,n}^0 - \phi_i^0\phi_{7,n\theta}^0$ is zero. Then, since $\phi_{,\theta}^I = -\phi_{,\beta}^I$,

$$I_X^2 = 2\mathrm{i}K\frac{\partial^2}{\partial\beta\partial K}\int_{S_R}(\phi^I\phi_{i,n}^0 - \phi_i^0\phi_{,n}^I)\mathrm{d}S. \tag{6.10}$$

Comparing with (6.4), we find that $I_X^2 = -\int_{S_B}\phi_7^{11}\phi_{i,n}^0\mathrm{d}S$.

Finally, we consider the integral over S_F in (6.6). By applying the boundary conditions at the free surface for the potentials involved, Green's theorem, the boundary conditions for $\boldsymbol{w}$ at S_B and S_R, and that S_B is wall-sided at $z = 0$, we find

$$\int_{S_F}(\psi_7^1\phi_{i,n}^0 - \phi_i^0\psi_{7,n}^1 + \psi_i^1\phi_{D,n}^0 - \phi_D^0\psi_{i,n}^1)\mathrm{d}S$$
$$= 2\mathrm{i}K\int_{S_F}\nabla_h\cdot(\boldsymbol{w}\phi_i^0\phi_D^0)\mathrm{d}S = 2\mathrm{i}K\int_{C_B+C_R}\phi_i^0\phi_D^0\boldsymbol{w}\cdot\boldsymbol{n}\,\mathrm{d}l = 0 \tag{6.11}$$

where C_B and C_R denote the mean water line of S_B and S_R, respectively.

Thus, $X_i^1/\rho g = I_X^3$. By carrying out the integration in (6.8), applying (3.28) and the method of stationary phase, we obtain

$$\frac{X_i^1}{\rho g} = -\left(\frac{2\pi}{k}\right)^{1/2}C_g(kh)H_i^{13}(\beta+\pi)\mathrm{e}^{\mathrm{i}\pi/4}, \qquad i = 1,\ldots,6. \tag{6.12}$$

Generalized Haskind relations are also derived for a body of general shape moving with a small forward speed (Nossen *et al.* 1991; Grue & Biberg 1993).

In figure 1 we show the exciting force $\mathrm{i}X_{i,\beta}^0 + X_i^1$ in heave and pitch for a ship. The force is obtained by both pressure integration and the generalized Haskind relation, with good agreement between the two different methods. Computations with coarser discretizations indicate convergence towards results between the solid and dashed lines. The largest relative computational error of about 5% occurs for $kl \simeq 14$ in figure 1(*b*). Otherwise the error is smaller. For comparison we also show the corresponding components $|X_i^0|$ of the exciting force (figure 1*e*, *f*), which are much smaller than $|\mathrm{i}X_{i,\beta}^0 + X_i^1|$ in these examples. As geometry we choose a ship oriented along the x-axis with section given by a half-circle and beam $b(x) = b_0[1-(2x/l)^4]$ for $|x| < l/2$, where the length to beam ratio is $l/b_0 = 5.6$, hereafter referred to as Ship 1. Working with a simple geometry allows for quite easy convergence tests. The length to beam ratio of Ship 1 corresponds to that of a Turret Production Ship (TPS) which is considered in some examples later (model shown in Grue & Palm 1993, figure 1).

6.2. *Added mass and damping*

By next setting the wave amplitude equal to zero ($A = 0$) we obtain the components of the force and moment in the radiation problem, i.e.

$$F_i^{rad} = -\rho\int_{S_B}\left(\frac{\partial\Phi}{\partial t} + \Omega\boldsymbol{w}\cdot\nabla\Phi\right)n_i\mathrm{d}S. \tag{6.13}$$

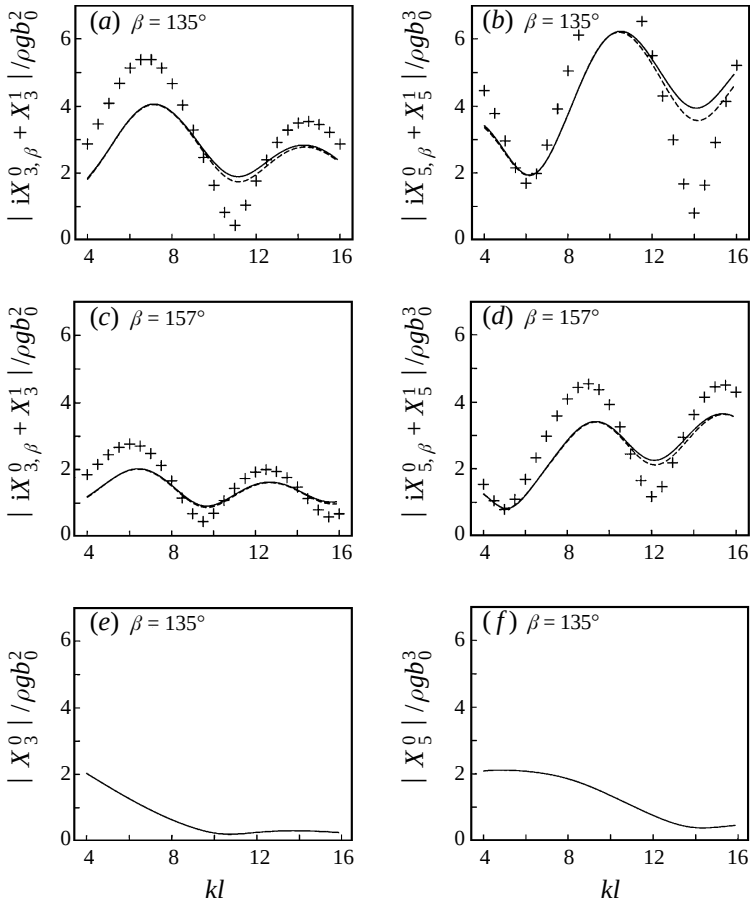

FIGURE 1. Exciting force in heave and pitch for Ship 1, 3136 panels on S_B and 12544 panels on S_F. Solid line, generalized far-field Haskind relations. Dashed line, pressure integration. Plus symbols, $|X_i^1|$ computed by the Haskind relations. In (*e*) and (*f*) we show, for comparison, $|X_i^0|$. $h = \infty$.

Expanding the integrand as

$$-\left(\frac{\partial \Phi}{\partial t} + \Omega \boldsymbol{w} \cdot \nabla \Phi\right) = \mathrm{Re}\left\{\rho\omega^2 \mathrm{e}^{\mathrm{i}\omega t}\left[\xi_j^0 \phi_j^0 + \epsilon\left(\xi_j^1 \phi_j^0 + 2\mathrm{i}\frac{\partial \xi_j^0}{\partial \beta}\frac{\partial}{\partial K}(K\phi_j^0) + \xi_j^0(\psi_j^1 - \mathrm{i}\boldsymbol{w}\cdot\nabla\phi_j^0)\right)\right]\right\} \quad (6.14)$$

motivates introducing

$$f_{ij}^0 = \rho\int_{S_B} \phi_j^0 n_i \mathrm{d}S, \qquad f_{ij}^1 = \rho\int_{S_B} (\psi_j^1 - \mathrm{i}\boldsymbol{w}\cdot\nabla\phi_j^0) n_i \mathrm{d}S, \quad (6.15)$$

where f_{ij}^0 and f_{ij}^1 contain the added mass and damping coefficients. We then find

$$F_i^{rad} = \mathrm{Re}\left\{\omega^2 e^{\mathrm{i}\omega t}\left[\xi_j^0 f_{ij}^0 + \epsilon\left(\xi_j^1 f_{ij}^0 + 2\mathrm{i}\frac{\partial \xi_j^0}{\partial \beta}\frac{\partial}{\partial K}(K f_{ij}^0) + \xi_j^0 f_{ij}^1\right)\right]\right\}. \quad (6.16)$$

The added mass and damping coefficients obey the well-known symmetry relations

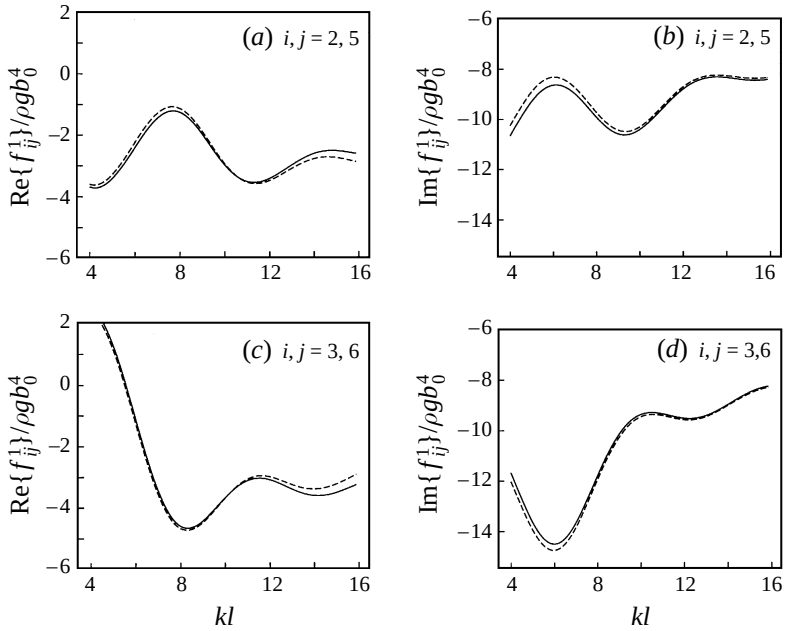

FIGURE 2. Comparison of f^1_{ij} (solid line) and $-f^1_{ji}$ (dashed line). Ship 1, 3136 panels on S_B and 12544 panels on S_F. $h = \infty$.

$f^0_{ij} = f^0_{ji}$ when $\Omega = 0$. For slender ships with forward speed, the added mass and damping coefficients obey the Timman–Newman symmetry relations. These relations have been generalized to also be valid for bodies of general shape under the restriction of a small forward speed (Wu & Eatock Taylor 1990; Nossen *et al.* 1991; Grue & Biberg 1993). It is possible to generalize the Timman–Newman relations to the present case also.

We consider the sum $f^1_{ij} + f^1_{ji}$. By using the variant of Stokes theorem (5.10), with G^0 replaced by ϕ^0_j, and using the body boundary condition for ψ^1_j, we find

$$f^1_{ij} + f^1_{ji} = \rho \int_{S_B} (\psi^1_j \phi^0_{i,n} - \phi^0_i \psi^1_{j,n} + \psi^1_i \phi^0_{j,n} - \phi^0_j \psi^1_{i,n}) \mathrm{d}S. \tag{6.17}$$

This integral may by use of Green's theorem be converted to integrals over S_F and S_R with the same integrand, but multiplied by -1. The integral over S_R becomes

$$-\rho \int_{S_R} (\psi^1_j \phi^0_{i,n} - \phi^0_i \psi^1_{j,n} + \psi^1_i \phi^0_{j,n} - \phi^0_j \psi^1_{i,n}) \mathrm{d}S. \tag{6.18}$$

By using the far-field conditions for ϕ^0_i and ψ^1_i (see (3.27) and (3.30)), the equation (6.18) may be written $\rho \int_{S_R} [\partial(\phi^0_i \phi^0_j)/\partial\theta] \mathrm{d}S$, which equals zero. The integral over S_F, i.e.

$$\rho \int_{S_F} (\psi^1_j \phi^0_{i,n} - \phi^0_i \psi^1_{j,n} + \psi^1_i \phi^0_{j,n} - \phi^0_j \psi^1_{i,n}) \mathrm{d}S, \tag{6.19}$$

becomes zero by using the same argument as in (6.11). We have then shown that

$$f^1_{ij} = -f^1_{ji}. \tag{6.20}$$

Numerical examples of the cross-coupling coefficients between sway and pitch, f^1_{25},

$-f^1_{52}$, and between heave and yaw, f^1_{36},$-f^1_{63}$, for Ship 1 illustrate that $f^1_{ij} \simeq -f^1_{ji}$, in agreement with the theory (figure 2). We note that the cross-coupling coefficients f^1_{35}, f^1_{53}, between heave and pitch become zero. We have also arrived at this result for the TPS (results not shown). For the symmetric Ship 1 we also have $f^0_{35} = f^0_{53} = 0$ in all the computations. The zero-speed cross-coupling coefficients f^0_{35}, f^0_{53} are different from zero for the TPS (results not shown), however.

6.3. *Equation of motion and body responses*

Balance of linear and angular momentum for the body gives

$$(F_1, F_2, F_3)\mathrm{e}^{\mathrm{i}\omega t} - 2\Omega \int_{m_b} \boldsymbol{k} \times \frac{\mathrm{d}\tilde{\boldsymbol{B}}}{\mathrm{d}t}\mathrm{d}m = \int_{m_b} \frac{\mathrm{d}^2\tilde{\boldsymbol{B}}}{\mathrm{d}t^2}\mathrm{d}m, \tag{6.21}$$

$$(F_4, F_5, F_6)\mathrm{e}^{\mathrm{i}\omega t} - 2\Omega \int_{m_b} \boldsymbol{x} \times \left(\boldsymbol{k} \times \frac{\mathrm{d}\tilde{\boldsymbol{B}}}{\mathrm{d}t}\right)\mathrm{d}m = \int_{m_b} \boldsymbol{x} \times \frac{\mathrm{d}^2\tilde{\boldsymbol{B}}}{\mathrm{d}t^2}\mathrm{d}m, \tag{6.22}$$

where the integration is over the body mass (m_b), and where (F_1, F_2, F_3) and (F_4, F_5, F_6) account for the sum of linear pressure forces, gravity and eventual mooring forces. The second term on the left is due to the Coriolis force.

The inertia terms on the right are represented by the usual mass matrix M_{ij} times the motion. By evaluating $\mathrm{d}^2\tilde{\boldsymbol{B}}/\mathrm{d}t^2$ we find for the right-hand sides of (6.21)–(6.22): $-\omega^2 M_{ij}\mathrm{Re}[(\xi^0_j + \epsilon(2\mathrm{i}\xi^0_{j,\beta} + \xi^1_j))\mathrm{e}^{\mathrm{i}\omega t}]$. The terms due to the Coriolis force may be represented similarly, i.e.

$$-2\mathrm{i}\epsilon\omega^2 M^c_{ij}\mathrm{Re}(\xi^0_j \mathrm{e}^{\mathrm{i}\omega t}), \tag{6.23}$$

where the matrix M^c_{ij} is given by

$$M^c_{ij} = \begin{pmatrix} 0 & -m_b & 0 & m_b Z_G & 0 & -m_b X_G \\ m_b & 0 & 0 & 0 & m_b Z_G & -m_b Y_G \\ 0 & 0 & 0 & 0 & 0 & 0 \\ -m_b Z_G & 0 & 0 & 0 & -I_{xy} & D_{yz} \\ 0 & -m_b Z_G & 0 & I_{xy} & 0 & -D_{xz} \\ m_b X_G & m_b Y_G & 0 & -D_{yz} & D_{xz} & 0 \end{pmatrix} \tag{6.24}$$

and (X_G, Y_G, Z_G) denotes centre of gravity, $I_{xy} = \int_{m_b} z^2\mathrm{d}m$, $D_{x_i x_j} = \int_{m_b} x_i x_j \mathrm{d}m$, moment of inertia and centrifugal moments, respectively. By using (6.3) for F^{ex}_i and (6.16) for F^{rad}_i, we find that the equation of motion becomes, to order ϵ^0 and ϵ^1, respectively

$$(-\omega^2(M_{ij} + f^0_{ij}) + c_{ij})\xi^0_j = AX^0_i, \tag{6.25}$$

$$(-\omega^2(M_{ij} + f^0_{ij}) + c_{ij})\xi^1_j = A(X^1_i + \mathrm{i}X^0_{i,\beta}) + \omega^2[(f^1_{ij} - 2\mathrm{i}M^c_{ij})\xi^0_j + 2\mathrm{i}(M_{ij} + (Kf^0_{ij})_{,K})\xi^0_{j,\beta}]. \tag{6.26}$$

Here, c_{ij} contain the coefficients of hydrostatic forces plus eventual mooring forces.

It is of interest to identify the frequencies of the responses of the floating body. We analyse this point in the following way. First we write the oscillatory responses $\mathrm{Re}(\xi_j \mathrm{e}^{\mathrm{i}\omega t}) = |\xi_j|\mathrm{Re}(\mathrm{e}^{\mathrm{i}\omega t + \mathrm{i}\delta_j})$, where the phase angle is determined by $\delta_j = \mathrm{Im}\ln\xi_j$, $(\xi_j \neq 0)$. The frequency of oscillation of mode number j is then given by

$$\frac{\mathrm{d}}{\mathrm{d}t}(\omega t + \delta_j) = \omega + \frac{\mathrm{d}\delta_j}{\mathrm{d}t} = \omega - \Omega\frac{\partial\delta^0_j}{\partial\beta} = \omega - \Omega\mathrm{Im}\left(\frac{1}{\xi^0_j}\frac{\partial\xi^0_j}{\partial\beta}\right) \qquad (\xi^0_j \neq 0) \tag{6.27}$$

to first order in ϵ.

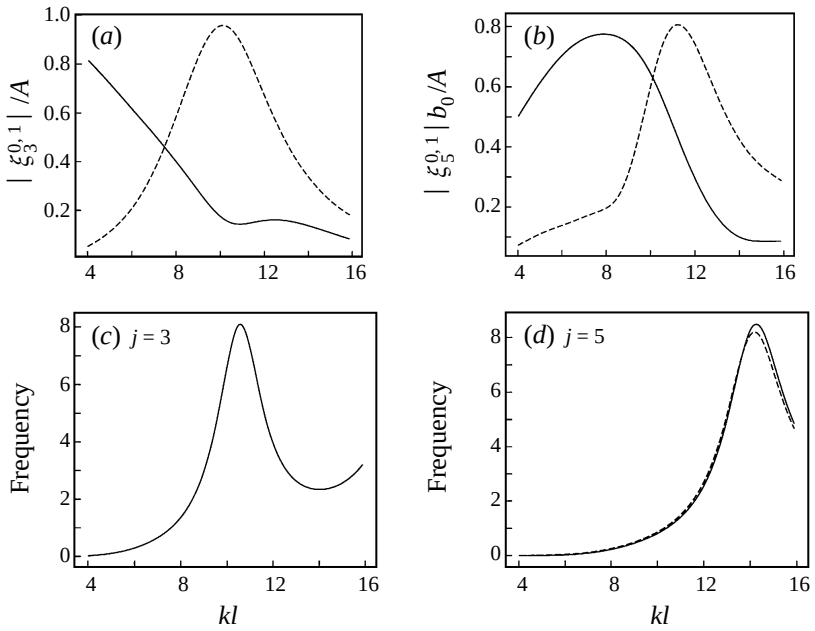

FIGURE 3. (a,b) The body response $|\xi_j^0|$ (solid line), and $|\xi_j^1|$ (dashed line) in heave and pitch. $|\xi_j^1|$ is scaled by a factor 0.1. (c,d) The first-order frequencies of oscillation $\mathrm{Im}\{(1/\xi_j^0)(\partial\xi_j^0/\partial\beta)\}$ (solid line, and $\mathrm{Im}\{(1/X_j^0)(\partial X_j^0/\partial\beta)\}$ (dashed line), also in heave and pitch. All curves are for Ship 1, 1600 panels on S_B and 6400 panels on S_F. $\beta = 135^\circ$. $h = \infty$.

Likewise, the frequency of oscillation of, say, the exciting force $\mathrm{Re}(X_j e^{i\omega t})$, is determined by

$$\sigma_{X_j} = \omega - \Omega \mathrm{Im}\left(\frac{1}{X_j^0}\frac{\partial X_j^0}{\partial \beta}\right) \qquad (X_j^0 \neq 0). \tag{6.28}$$

Examples of the responses in the vertical modes of motion of Ship 1 and the TPS in slow rotation are given in figures 3 and 4. We find that ξ_3^1, ξ_5^1 are much larger than their counterparts at $\Omega = 0$. Furthermore, both figures show that the frequency becomes different in the heave and pitch modes of motion. For Ship 1 the frequencies of the response and the exciting force are the same in the respective modes, practically speaking, while for the TPS the exciting force X_3 and the response ξ_3 have different frequencies (figure 4*c*). For this ship, the frequency of X_3 becomes large (but finite) for kl close to 9.2, which is because $|X_3^0|$ is very small close to this wavenumber. Corresponding results apply to the frequencies of ξ_5 and X_5 when kl is close to 13.5.

The properties of the surge motion due to a rotating Ship 1 for wave heading varying between 0° and 180° at a fixed wavenumber is also investigated, for the purpose of further illustration, see figure 5. Of interest, among others, is to see how the frequency of oscillation behaves for wave heading close to 90° (beam seas), where the surge motion disappears. The phase δ_1^0 jumps at this wave heading, without, however, affecting the derivative of δ_1^0 with respect to the wave angle, when β tends to 90° from above or below. Even $\partial\delta_1^0/\partial\beta = \mathrm{Im}[(\partial\xi_1^0/\partial\beta)/\xi_1^0]$ is smooth and becomes zero for $\beta \to 90^\circ$, in spite of $1/\xi_1^0$ becoming infinitely large there.

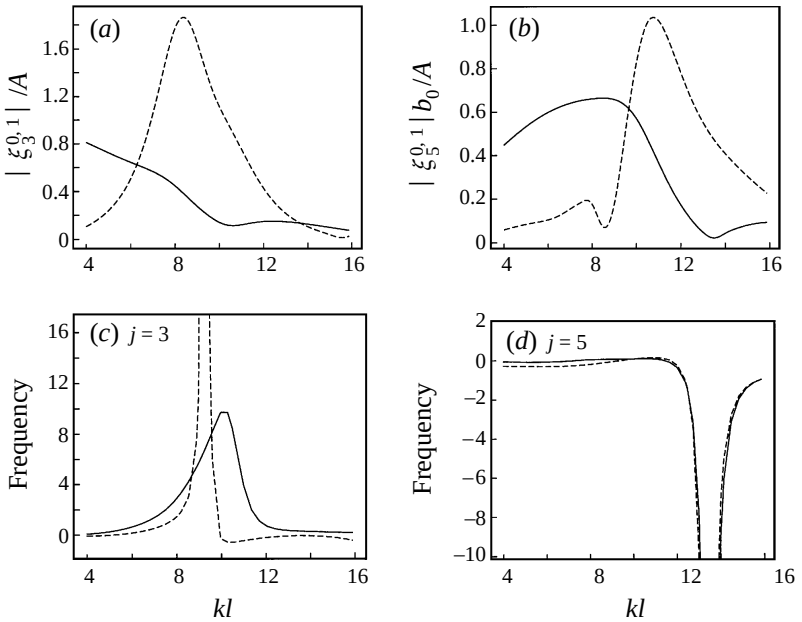

FIGURE 4. As figure 3, but for the TPS, 760 panels on S_B and 1800 panels on S_F.

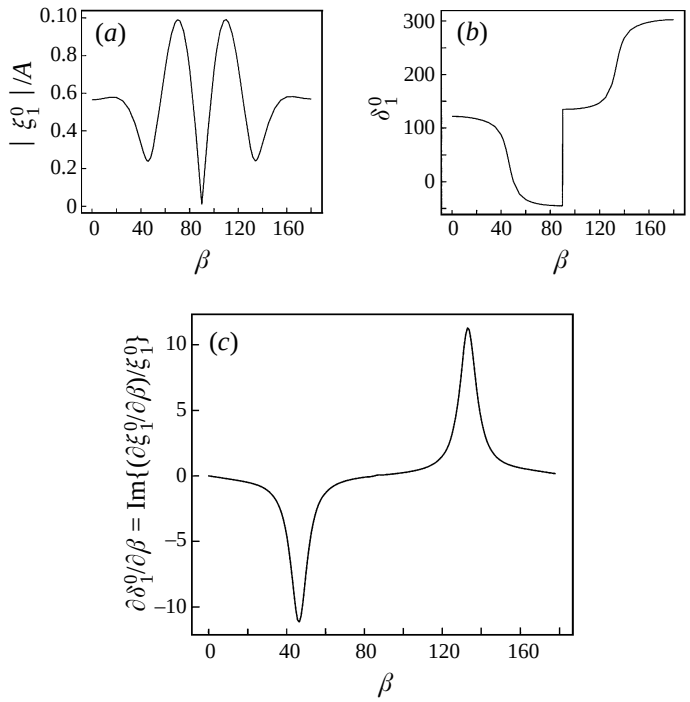

FIGURE 5. The surge mode of motion as a function of the wave angle: (*a*) The body response for $\Omega = 0$, (*b*) the phase angle, (*c*) the first-order frequency of oscillation. All curves are for Ship 1, 1568 panels on S_B and 6272 panels on S_F. $kl = 12.6$. $h = \infty$.

7. Wave-drift damping

The coefficients of the wave-drift damping matrix due to a slow angular velocity are now considered. We outline here only the new steps required in the complete radiation–diffraction problem, which are not covered by the diffraction analyses by Newman (1993), GP and Grue (1996). We denote the time-averaged horizontal force by $\overline{\boldsymbol{F}} = \overline{F}_1\boldsymbol{i}_1 + \overline{F}_2\boldsymbol{i}_2$ ($\boldsymbol{i}_1 = \boldsymbol{i}, \boldsymbol{i}_2 = \boldsymbol{j}$) and the time-averaged moment about the vertical axis by $\overline{M}_6$. The wave-drift damping coefficients appear by expanding $\overline{F}_1, \overline{F}_2, \overline{M}_6$ in perturbation series in the angular velocity, i.e.

$$(\overline{F}_1, \overline{F}_2, \overline{M}_6) = (F_{10}, F_{20}, M_{60}) - \epsilon(B_{16}, B_{26}, B_{66}) \tag{7.1}$$

where F_{10}, F_{20}, M_{60} denote the forces and moment when $\epsilon = 0$ and the last term, proportional to the slow yaw velocity, is a generalized damping term. The coefficients B_{16}, B_{26}, B_{66} comprise the part of the wave-drift damping matrix due to the slow angular motion. Following GP for the diffraction problem, we apply conservation of linear and angular momentum to derive formulae for B_{i6}, accounting for terms proportional to the wave amplitude squared times the slow velocity, disregarding higher-order terms.

7.1. *The forces* B_{16}, B_{26}

Conservation of linear momentum gives

$$\overline{\boldsymbol{F}} = \epsilon\rho\omega\left(\boldsymbol{i}_i\frac{\partial}{\partial\beta} - \boldsymbol{k}\times\boldsymbol{i}_i\right)\overline{\int_V \Phi'_{,x_i}\mathrm{d}V} - \boldsymbol{i}_i\overline{\int_{S_R}(pn_i + \rho\Phi'_{,x_i}\nabla\Phi'\cdot\boldsymbol{n})\mathrm{d}S} \tag{7.2}$$

where a bar denotes time-average, and V the (time-dependent) fluid volume bounded by the vertical circular cylinder S_R, the (moving) free surface and the (moving) body boundary, and the sum over $i = 1, 2$ is understood. The integral $\overline{\int_V \Phi'_{,x_i}\mathrm{d}V}$ contains, in the complete radiation–diffraction problem, some new terms due to the body motions. By evaluating the time average we find

$$\overline{\int_V \Phi'_{,x_i}\mathrm{d}V} = \int_{S_B}\overline{\Phi_{,x_i}\tilde{\boldsymbol{B}}\cdot\boldsymbol{n}}\mathrm{d}S + \int_{S_F}\overline{\Phi_{,x_i}\zeta}\mathrm{d}S + \int_{\mathscr{V}}\psi^{(2)}_{,x_i}\mathrm{d}V, \tag{7.3}$$

where $\tilde{\boldsymbol{B}}$ is given in (3.14), ζ denotes the free-surface elevation and the integration on the right is over the mean positions of the wetted body surface, the free surface and the fluid volume, S_B, S_F, $\mathscr{V}$, respectively. Since $\overline{\int_V \Phi'_{,x_i}\mathrm{d}V}$ appears in (7.2) multiplied by ϵ, it suffices to evaluate (7.3) to $O(A^2)$. Introducing $\Phi = \mathrm{Re}\{(\mathrm{i}Ag/\omega)\phi^0\mathrm{e}^{\mathrm{i}\omega t}\}$ we find

$$\overline{\int_V \Phi'_{,x_i}\mathrm{d}V} = \frac{gA^2}{2\omega}\mathrm{Im}\int_{S_B}\boldsymbol{B}^0\cdot\boldsymbol{n}\phi^{0*}_{,x_i}\mathrm{d}S + \frac{gA^2}{2\omega}\mathrm{Im}\int_{S_F}\phi^0\phi^{0*}_{,x_i}\mathrm{d}S + \int_{S_B}\psi^{(2)}n_i\mathrm{d}S + \int_{S_R}\psi^{(2)}n_i\mathrm{d}S \quad (i = 1, 2) \tag{7.4}$$

where $\boldsymbol{B}^0$ is given after (4.2) and we have used Gauss' theorem to obtain the two last terms on the right of (7.4).

We proceed by rewriting the second and third terms on the right of (7.4). By using Gauss' theorem we find for the second term

$$\mathrm{Im}\int_{S_F}\phi^0\phi^{0*}_{,x_i}\mathrm{d}S = \mathrm{Im}\int_{S_F}x_i\phi^0\phi^{0*}_{,zz}\mathrm{d}S + \mathrm{Im}\int_{C_B+C_R}x_i\phi^0\phi^{0*}_{,n}\mathrm{d}S. \tag{7.5}$$

To rewrite the third term on the right of (7.4) we introduce the auxiliary potentials

χ_1, χ_2 satisfying $\nabla^2\chi_i$ in the fluid, $\chi_{i,n} = n_i$ at S_B, $\chi_{i,z} = 0$ at $z = 0, -h$, $|\nabla\chi_i| \to 0$, $R \to \infty$. Applying Green's theorem to $\psi^{(2)}$ and χ_i we find

$$\int_{S_B} \psi^{(2)} n_i \mathrm{d}S = \int_{S_B+S_F} \chi_i \psi^{(2)}_{,n} \mathrm{d}S. \tag{7.6}$$

Inserting the boundary conditions for $\psi^{(2)}$ at S_F and at S_B, see (4.1)–(4.2), gives

$$\int_{S_F} \chi_i \psi^{(2)}_{,z} \mathrm{d}S = -\frac{gA^2}{2\omega} \mathrm{Im} \int_{S_F} \chi_i \phi^0 \phi^{0*}_{,zz} \mathrm{d}S, \tag{7.7}$$

$$\int_{S_B} \chi_i \psi^{(2)}_{,n} \mathrm{d}S = \frac{gA^2}{2\omega} \mathrm{Im} \int_{S_B} \chi_i \{ \boldsymbol{B}^0 \cdot (\boldsymbol{n} \cdot \nabla) \nabla \phi^{0*} - \boldsymbol{C}^0 \cdot (K \boldsymbol{B}^{0*} - \nabla \phi^{0*}) \} \mathrm{d}S \tag{7.8}$$

where $\boldsymbol{C}^0$ is defined after (4.2). The integral over $\chi_i \boldsymbol{B}^0 \cdot (\boldsymbol{n} \cdot \nabla) \nabla \phi^{0*}$ in (7.8) may be simplified, and we proceed as follows: First we use a variant of Stokes' theorem (GP, equation B3), giving

$$\begin{aligned} \int_{S_B} \chi_i \boldsymbol{B}^0 \cdot (\boldsymbol{n} \cdot \nabla) \nabla \phi^{0*} \mathrm{d}S = & \int_{S_B} \{ \boldsymbol{n} \cdot (\nabla \phi^{0*} \cdot \nabla)(\chi_i \boldsymbol{B}^0) + K \boldsymbol{B}^0 \cdot \boldsymbol{n} \nabla \cdot (\chi_i \boldsymbol{B}^{0*}) \} \mathrm{d}S \\ & - \int_{C_B} \chi_i K \boldsymbol{B}^0 \cdot \boldsymbol{n} (\phi^{0*} + \boldsymbol{k} \cdot \boldsymbol{B}^{0*}) \mathrm{d}l. \end{aligned} \tag{7.9}$$

Next we note that $\nabla \cdot \boldsymbol{B}^0 = 0$ and that $\boldsymbol{n} \cdot (\nabla \phi^{0*} \cdot \nabla)(\chi_i \boldsymbol{B}^0) = \boldsymbol{B}^0 \cdot \boldsymbol{n} \nabla \chi_i \cdot \nabla \phi^{0*} - \chi_i \boldsymbol{C}^0 \cdot \nabla \phi^{0*}$, which means that (7.8) becomes

$$\int_{S_B} \chi_i \psi^{(2)}_{,n} \mathrm{d}S = \frac{gA^2}{2\omega} \mathrm{Im} \left(- \int_{S_B} \boldsymbol{B}^0 \cdot \boldsymbol{n} \nabla \chi_i \cdot \nabla \phi^{0*} \mathrm{d}S + \int_{C_B} K \boldsymbol{B}^0 \cdot \boldsymbol{n} \chi_i \phi^{0*} \mathrm{d}l \right) + I, \tag{7.10}$$

where

$$I = \frac{\omega A^2}{2} \mathrm{Im} \left(\int_{C_B} \boldsymbol{B}^0 \cdot \boldsymbol{n} \boldsymbol{k} \cdot \boldsymbol{B}^{0*} \chi_i \mathrm{d}l - \int_{S_B} \boldsymbol{B}^0 \cdot \boldsymbol{n} \boldsymbol{B}^{0*} \cdot \nabla \chi_i \mathrm{d}S + \int_{S_B} \boldsymbol{B}^{0*} \cdot \boldsymbol{C}^0 \chi_i \mathrm{d}S \right). \tag{7.11}$$

We may show that $I = 0$. The first and second terms of (7.11) give

$$\begin{aligned} \mathrm{Im} \left(\int_{C_B} \boldsymbol{B}^0 \cdot \boldsymbol{n} \boldsymbol{k} \cdot \boldsymbol{B}^{0*} \chi_i \mathrm{d}l - \int_{S_B} \boldsymbol{B}^0 \cdot \boldsymbol{n} \boldsymbol{B}^{0*} \cdot \nabla \chi_i \mathrm{d}S \right. &= \frac{1}{2} \int_{C_B} (\boldsymbol{B}^0 \times \boldsymbol{B}^{0*}) \cdot (\boldsymbol{n} \times \boldsymbol{k}) \chi_i \mathrm{d}l \\ \left. - \frac{1}{2} \int_{S_B} (\boldsymbol{B}^0 \times \boldsymbol{B}^{0*}) \cdot (\boldsymbol{n} \times \nabla \chi_i) \mathrm{d}S = \frac{1}{2} \int_{S_B} \chi_i \nabla \times (\boldsymbol{B}^0 \times \boldsymbol{B}^{0*}) \mathrm{d}S \right), \end{aligned} \tag{7.12}$$

where we have used Stokes' theorem in the last step. By then expanding the integrand on the right we find that (7.12) is equal to $-\mathrm{Im} \int_{S_B} \boldsymbol{B}^{0*} \cdot \boldsymbol{C}^0 \chi_i \mathrm{d}S$, which gives that $I = 0$.

We then obtain

$$\overline{\int_V \Phi'_{,x_i} \mathrm{d}V} = \frac{gA^2}{\omega} \left(M_i + \tfrac{1}{2} \mathrm{Im} \int_{C_R} x_i \phi^0 \phi^{0*}_{,n} \mathrm{d}l \right) + \int_{S_R} \psi^{(2)} n_i \mathrm{d}S, \tag{7.13}$$

where

$$\begin{aligned} M_i = \tfrac{1}{2} \mathrm{Im} \left(- \int_{S_B} \right. & \boldsymbol{B}^0 \cdot \boldsymbol{n} \nabla (\chi_i - x_i) \cdot \nabla \phi^{0*} \mathrm{d}S \\ & \left. + K \int_{C_B} (\chi_i - x_i) \boldsymbol{B}^0 \cdot \boldsymbol{n} \phi^{0*} \mathrm{d}l - \int_{S_F} (\chi_i - x_i) \phi^0 \phi^{0*}_{,zz} \mathrm{d}S \right). \end{aligned} \tag{7.14}$$

By applying (7.7) and (7.10), with χ_i replaced by $\chi_i - x_i$, we also have

$$M_i = (\omega/gA^2)\int_{S_B+S_F}(\chi_i - x_i)\psi^{(2)}_{,n}\mathrm{d}S.$$

We note that the potential $\psi^{(2)}$ may be obtained as a multipole expansion of a source potential between the rigid walls at $z = 0, -h$, and we may show that M_1, M_2 determine the dipole moments in this expansion, see also Grue & Palm (1993).

The last term in (7.2) becomes, following GP,

$$-\overline{\int_{S_R}(pn_i + \rho\Phi'_{,x_i}\nabla\Phi'\cdot\boldsymbol{n})\mathrm{d}S} = \frac{\rho gA^2}{4K}\int_{S_R}\mathrm{Re}\{\phi(\phi^*_{,x_i})_{,n} - \phi_{,x_i}\phi^*_{,n}\}\mathrm{d}S - \epsilon\rho\omega\int_{S_R}(\psi^{(2)}_{,\beta} + \psi^{(2)}_{,\theta})n_i\mathrm{d}S, \quad (7.15)$$

where $\Phi' = \mathrm{Re}\{(\mathrm{i}Ag/\omega)\phi\mathrm{e}^{\mathrm{i}\omega t}\} + \Omega\chi_6 + \psi^{(2)}$ is used. We then introduce (7.13) and (7.15) into (7.1)–(7.2), and expand $\phi = \phi^0 + \epsilon\phi^1$ in (7.15), where

$$\phi^0 = \phi^0_D + K(\xi^0_j/A)\phi^0_j, \quad (7.16)$$

$$\phi^1 = 2\mathrm{i}K\frac{\partial^2\phi^0}{\partial K\partial\beta} + 2\mathrm{i}K\frac{\partial^2\phi^0}{\partial K\partial\theta} + \phi^{13}, \quad (7.17)$$

$$\phi^{13} = \phi^{13}_7 + K\left[\left(\xi^1_j + \mathrm{i}\frac{\partial\xi^0_j}{\partial\beta} - 2\mathrm{i}\frac{\partial^2(K\xi^0_j)}{\partial K\partial\beta}\right)\phi^0_j - 2\mathrm{i}\frac{\partial(K\xi^0_j)}{\partial K}\frac{\partial\phi^0_j}{\partial\theta} + \xi^0_j\phi^{13}_j\right]\Big/A. \quad (7.18)$$

By also applying the far-field forms

$$\phi^0 - \phi^I = R^{-1/2}H^0(\theta)Ch(kz)\mathrm{e}^{-\mathrm{i}kR}(1 + O((kR)^{-1})), \quad (7.19)$$

$$\phi^{13} = R^{-1/2}H^{13}(\theta)Ch(kz)\mathrm{e}^{-\mathrm{i}kR}(1 + O((kR)^{-1})) \quad (7.20)$$

we find after some algebra

$$\frac{B_{i6}\boldsymbol{i}_i}{\rho gA^2} = -\left(\boldsymbol{i}_i\frac{\partial}{\partial\beta} - \boldsymbol{k}\times\boldsymbol{i}_i\right)M_i + \frac{1}{2}\int_0^{2\pi}\mathrm{Re}\left\{H^0(\theta)H^{1*}(\theta)\begin{pmatrix}\cos\theta\\ \sin\theta\end{pmatrix} - 2\mathrm{i}H^0(\theta)\left[H^0_{,\beta\theta}(\theta) + H^0_{,\theta\theta}(\theta)\right]^*\begin{pmatrix}-\sin\theta\\ \cos\theta\end{pmatrix}\right\}\mathrm{d}\theta + \frac{1}{2}\mathrm{Re}\left\{\left(\frac{2\pi}{k}\right)^{1/2}\mathrm{e}^{\mathrm{i}\pi/4}\left[H^{1*}(\beta)\begin{pmatrix}\cos\beta\\ \sin\beta\end{pmatrix} - 2\mathrm{i}\left[H^0_{,\beta\theta}(\beta) + H^0_{,\theta\theta}(\beta)\right]^*\begin{pmatrix}-\sin\beta\\ \cos\beta\end{pmatrix}\right]\right\}, \quad (7.21)$$

where

$$H^0 = H^0_7 + K(\xi^0_j/A)H^0_j, \quad (7.22)$$

$$H^1 = \frac{kC_g}{K}[2\mathrm{i}K(H^0_{,\beta K} + H^0_{,\theta K}) + H^{13}] + \frac{\mathrm{i}k}{C_g}\frac{\partial C_g}{\partial k}(H^0_{,\beta} + H^0_{,\theta}), \quad (7.23)$$

$$H^{13} = H^{13}_7 + K\left[\left(\xi^1_j + \mathrm{i}\frac{\partial\xi^0_j}{\partial\beta} - 2\mathrm{i}\frac{\partial^2(K\xi^0_j)}{\partial K\partial\beta}\right)H^0_j - 2\mathrm{i}\frac{\partial(K\xi^0_j)}{\partial K}\frac{\partial H^0_j}{\partial\theta} + \xi^0_jH^{13}_j\right]\Big/A. \quad (7.24)$$

The amplitudes H_j^0 and H_j^{13} are given in (5.15)–(5.16) and H_7^0 and H_7^{13} in (A 4)–(A 5). We note that H^0 and H^{13} are of forms corresponding to the potentials in (7.16) and (7.18), respectively. The amplitude H^1 is composed of two terms on the other hand, one term of a form like (7.17), and another term proportional to $\partial C_g/\partial k$. The latter term disappears when $h \to \infty$.

Equation (7.21) expresses B_{16} and B_{26} by the (far-field) dipole moments M_1, M_2 of the potential $\psi^{(2)}$ and the far-field amplitudes of the linear potentials. These formulae are valid for arbitrary constant water depth and arbitrary linear body responses, and generalize the formulae of Newman (1993) and GP, which were derived for the diffraction problem at infinite water depth. We note that (7.21) formally is of the same form as GP's equation (7.12), however with quite extended amplitude functions and dipole moments M_1, M_2 here.

7.2. *The moment* B_{66}

Conservation of angular momentum gives

$$\overline{M}_6 = \epsilon\rho\omega \frac{\partial}{\partial\beta} \overline{\int_V \Phi'_{,\theta} \mathrm{d}V} + \rho \overline{\int_{S_R} \Phi'_{,\theta} \nabla\Phi' \cdot \boldsymbol{n}) \mathrm{d}S}. \tag{7.25}$$

Similarly to (7.4) we find for the first integral on the right of (7.25)

$$\overline{\int_V \Phi'_{,\theta} \mathrm{d}V} = \frac{gA^2}{2\omega} \mathrm{Im}\left(\int_{S_B} \boldsymbol{B}^0 \cdot \boldsymbol{n} \phi^{0*}_{,\theta} \mathrm{d}S + \int_{S_F} \phi^0 \phi^{0*}_{,\theta} \mathrm{d}S \right) + \int_{S_B} \psi^{(2)} n_6 \mathrm{d}S. \tag{7.26}$$

The last term on the right of (7.26) may be rewritten similarly to (7.6)–(7.10), i.e.

$$\int_{S_B} \psi^{(2)} n_6 \mathrm{d}S = -\frac{gA^2}{2\omega} \mathrm{Im}\left(\int_{S_F} \chi_6 \phi^0 \phi^{0*}_{,zz} \mathrm{d}S + \int_{S_B} \boldsymbol{B}^0 \cdot \boldsymbol{n} \nabla\chi_6 \cdot \nabla\phi^{0*} \mathrm{d}S - K \int_{C_B} \boldsymbol{B}^0 \cdot \boldsymbol{n} \chi_6 \phi^{0*} \mathrm{d}l \right). \tag{7.27}$$

The second term on the right of (7.25) becomes

$$-\frac{\rho g A^2}{2K} \left(\int_{S_R} \mathrm{Re}\{\phi^0_{,\theta} \phi^{0*}_{,n}\} \mathrm{d}S + \epsilon \int_{S_R} \mathrm{Re}\{\phi^0_{,\theta} \phi^{1*}_{,n} + \phi^1_{,\theta} \phi^{0*}_{,n}\} \mathrm{d}S \right), \tag{7.28}$$

where we have inserted $\Phi' = \Phi = \mathrm{Re}\{(\mathrm{i}Ag/\omega)(\phi^0 + \epsilon\phi^1)\}$ and kept the leading terms. Inserting (7.25)-(7.28) into (7.1) we find

$$\frac{B_{66}}{\rho g A^2} = \frac{1}{2} \frac{\partial}{\partial\beta} \int_{S_B} \mathrm{Im}\{\boldsymbol{B}^0 \cdot \boldsymbol{n}\boldsymbol{w} \cdot \nabla\phi^{0*}\} \mathrm{d}S - \frac{K}{2} \frac{\partial}{\partial\beta} \int_{C_B} \mathrm{Im}\{\boldsymbol{B}^0 \cdot \boldsymbol{n} \chi_6 \phi^{0*}\} \mathrm{d}l + \frac{1}{2} \frac{\partial}{\partial\beta} \int_{S_F} \mathrm{Im}\{\chi_6 \phi^0 \phi^{0*}_{,zz} + \phi^0_{,\theta} \phi^{0*}\} \mathrm{d}S + \frac{1}{2K} \int_{S_R} \mathrm{Re}\{\phi^0_{,\theta} \phi^{1*}_{,n} + \phi^1_{,\theta} \phi^{0*}_{,n}\} \mathrm{d}S. \tag{7.29}$$

We may rewrite the sum of the second and third integrals in (7.29) as follows. First we exploit the boundary conditions for ϕ^0, ϕ^1 and χ_6 at S_B and S_F, and apply Gauss' theorem twice. We can show that this sum becomes

$$-\frac{1}{2K} \int_{S_F} Re\{\phi^{0*}_{,\beta} \phi^1_{,n} - \phi^1 \phi^{0*}_{,\beta n}\} \mathrm{d}S. \tag{7.30}$$

Next we apply Green's theorem to $\phi^0_{,\beta}$ and ϕ^1, and find that (7.30) may be recast into integrals over S_B and S_R, giving for B_{66}

$$\frac{B_{66}}{\rho g A^2} = \frac{1}{2K}\int_{S_B} \mathrm{Re}\{\phi^{0*}_{,\beta}\phi^1_{,n} - \phi^1\phi^{0*}_{,\beta n} - \frac{\partial}{\partial\beta}(\mathrm{i}K\boldsymbol{B}^0\cdot\boldsymbol{nw}\cdot\nabla\phi^{0*})\}\mathrm{d}S$$
$$+\frac{1}{2K}\int_{S_R}\mathrm{Re}\{(\phi^{0*}_{,\beta}+\phi^{0*}_{,\theta})\phi^1_{,n} - \phi^{1*}(\phi^0_{,\beta}+\phi^0_{,\theta})_{,n}\}\mathrm{d}S. \tag{7.31}$$

The integral over S_B in (7.31) may then be expressed in terms of the linear hydrodynamic forces, i.e.

$$\frac{1}{2K}\int_{S_B}\mathrm{Re}\{\phi^{0*}_{,\beta}\phi^1_{,n} - \phi^1\phi^{0*}_{,\beta n} - \frac{\partial}{\partial\beta}(\mathrm{i}K\boldsymbol{B}^0\cdot\boldsymbol{nw}\cdot\nabla\phi^{0*})\}\mathrm{d}S$$
$$= \frac{-1}{2\rho g A^2}\mathrm{Re}\left\{\xi^{0*}_{i,\beta}[A(X^1_i + X^0_{i,\beta}) - c_{ji}\xi^1_j + \omega^2((f^0_{ij}+M_{ji})\xi^1_j + f^1_{ij}\xi^0_j + 2i(Kf^0_{ij})_{,K}\xi^0_{j,\beta})]\right\} \tag{7.32}$$

where (5.10) and the equation of motion (6.25) have been used. We then apply (6.26) and that the body mass matrix M_{ij} is symmertic, finding that (7.32) becomes

$$\mathrm{Im}\Big(\omega^2 M^c_{ij}\xi^{0*}_{i,\beta}\xi^0_j + \mathrm{i}c_{ij}(\xi^{0*}_{j,\beta}\xi^1_i - \xi^{0*}_{i,\beta}\xi^1_j)/2\Big)/(\rho g A^2) \tag{7.33}$$

where (6.26) has been used.

By introducing the far-field form of the potentials ϕ^0 and ϕ^1 into the last term of (7.31) and evaluating the integrals we finally arrive at

$$\frac{B_{66}}{\rho g A^2} = \mathrm{Im}\left\{\frac{\omega^2 M^c_{ij}\xi^{0*}_{i,\beta}\xi^0_j}{\rho g A^2} + \frac{\mathrm{i}c_{ij}(\xi^{0*}_{j,\beta}\xi^1_i - \xi^{0*}_{i,\beta}\xi^1_j)}{2\rho g A^2} - \frac{1}{2k}\int_0^{2\pi}(H^0_{,\beta}(\theta)+H^0_{,\theta}(\theta))H^{1*}(\theta)\mathrm{d}\theta\right\}, \tag{7.34}$$

where H^0 and H^1 are determined by (7.22)–(7.23). In the coupled radiation–diffraction problem the formula for B_{66} contains two extra terms which are completely absent in the diffraction problem. The first term is expressed by the linear body responses and the matrix (6.24) representing the Coriolis force in the equation governing the linear motions. The second term involves the restoring force matrix c_{ij}. This term becomes zero when c_{ij} is symmetric, however. The formula for the wave-drift damping moment is valid for arbitrary water depth and arbitrary linear body motions. For the diffraction problem, the formulae for B_{66} by Newman (1993), GP and Grue (1996) are recovered.

7.3. *Numerical examples*

Computations of the wave-drift damping coefficients B_{i6} have been performed for the two ship models described in § 6.1, see figures 6–8. The wave angles are 90° (beam seas), 135° (quartering seas), 157°, 180° (head seas) and the wavenumber is in the range $4 < kl < 16$. For a ship with length $l = 230$ m the corresponding wavelength λ is in the interval $90 < \lambda < 360$ m. The computations show that B_{i6} not only depend on the length to beam ratio of a ship, but also on the detailed form of the ship geometry. This is an expected result, partly because the two geometries have different motion characteristics, see § 6.3, with correspondingly different contributions to the final formulae for the wave-drift damping coefficients and wave-drift force and moment. The results for the two ships may differ quite significantly for wave headings in the range between beam seas (90°) and quartering seas (135°), depending on the wavenumber. However, there are also some differences for wave headings close to 180°.

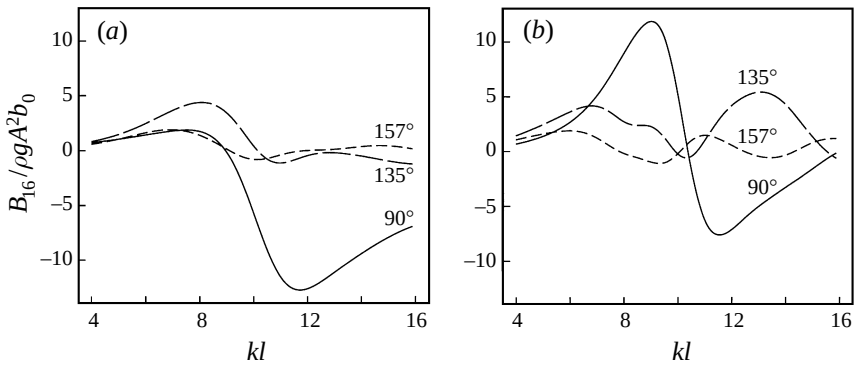

FIGURE 6. The damping coefficient B_{16} at different wave angles. (*a*) Ship 1, 1600 panels on S_B and 6400 panels on S_F. (*b*) The TPS, 760 panels on S_B and 1800 panels on S_F. $h = \infty$.

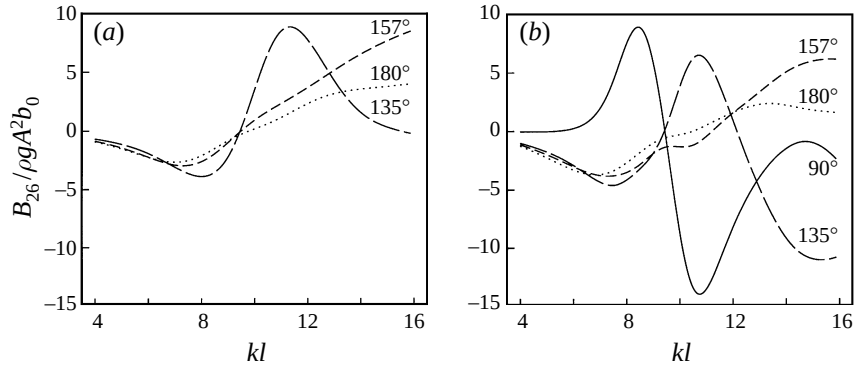

FIGURE 7. As figure 6, but for B_{26}.

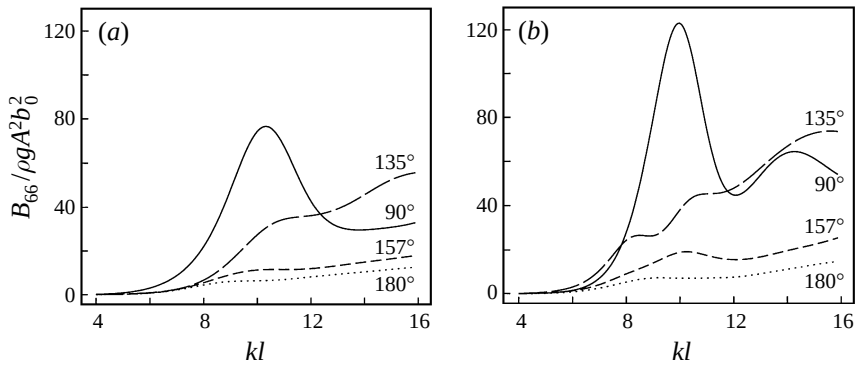

FIGURE 8. As figure 6, but for B_{66}.

We may compare computations of B_{i6} with and without radiation effects, where results for the latter were given in GP. Such a comparison shows that B_{i6}, with the complete radiation–diffraction effects included, are large for moderate wavelengths, and may have quite large peaks or rapid variations close to the resonances in the vertical modes of motion. For longer waves ($kl < 5$) B_{i6} are small. The results for the diffraction problem exhibit more monotonic behaviour of B_{i6} than for the complete radiation–diffraction problem.

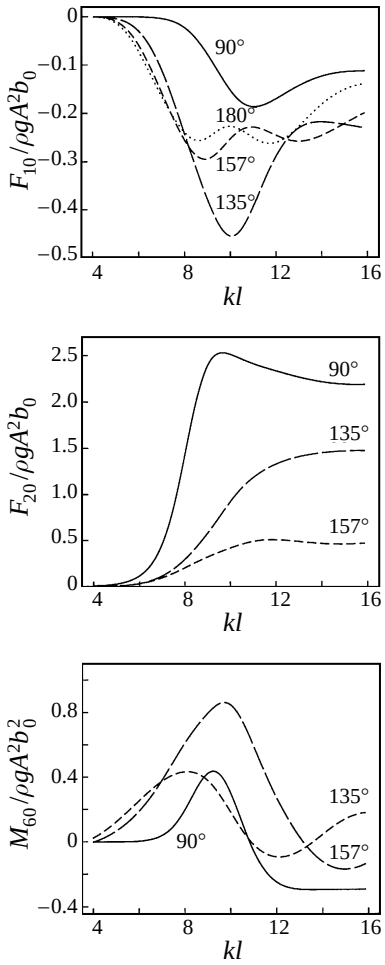

FIGURE 9. F_{10}, F_{20} and M_{60} at different wave angles. (180° means head waves.) The TPS, 760 panels on S_B. 1800 panels on S_F.

The computations exhibit a positive damping moment B_{66} for the two ship models. The damping also becomes larger for the TPS than for Ship 1, which is most pronounced in beam seas. The generalized damping forces B_{16} and B_{26} may become both positive and negative. There appear to be no physical reasons which contradict the latter results. The wave-drift damping computations are also compared with the forces and moment for $\epsilon = 0$, which are displayed in figure 9 for the TPS. We observe that the magnitude of B_{i6} is much larger than that of (F_{10}, F_{20}, M_{60}). We have, for example, that $B_{66}/M_{60} \simeq 300$ at the peak for $kl \simeq 10$ and $\beta = 90°$. Thus, even for very small $\epsilon = \Omega/\omega$ the effect of a rotation on the total moment may be rather large. A similar result applies to the longitudinal force $\overline{F}_1$. The effect of a rotation is somewhat smaller for the lateral force $\overline{F}_2$.

7.4. *Comparison with damping due to viscous effects*

It is of interest to compare wave-drift damping and viscous damping in the yaw mode of motion. There appears to be little published about the latter, so we here provide an estimate of viscous damping in the yaw mode from the sectionwise drag on the

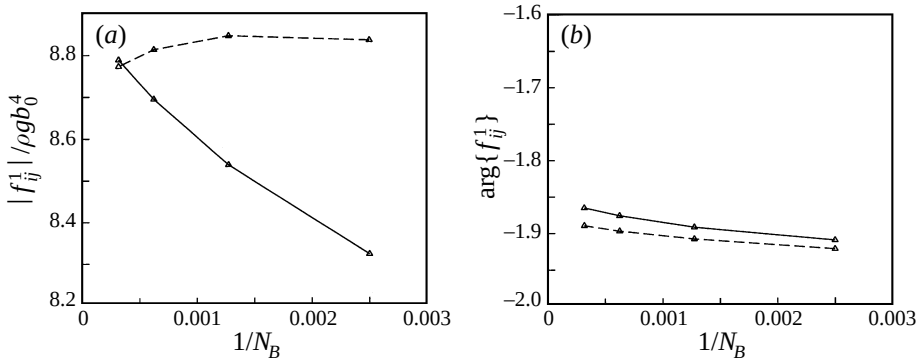

FIGURE 10. Convergence of f_{25}^1 (solid line) and $-f_{52}^1$ (dashed line) vs. N_B, the number of panels on S_B. Ship 1. $kl = 14.5$. $h = \infty$. $(N_B, N_F) = (3136, 12544)$, (1600, 6400), (784, 3136), (400, 1600).

ship. This is given by $\mathrm{d}D = (1/2)\rho C_D T(x)x|x|\Omega|\Omega|\mathrm{d}x$, where $T(x)$ is the sectionwise draught and the x-axis is in the length-direction of the ship. This local drag gives rise to a moment given by

$$M_{Visc} = \int_{-l/2}^{l/2} x\mathrm{d}D = (1/\gamma)\rho C_D \Omega|\Omega| b_0 l^4, \tag{7.35}$$

where $\gamma = 256$ for Ship 1 and $\gamma = 171$ for the TPS. A practical case concerning the slow yaw motions of a moored TPS is described in Faltinsen (1990, p. 280). The data in this case are: Ship length, $l = 230$ m, natural period of the yaw motion, 400 s, standard deviation of the slow yaw-angle, 3°. This means that the standard deviation of Ω is $8.22 \times 10^{-4}\mathrm{s}^{-1}$. The drag coefficient may be estimated by $C_D = 1$ (see Faltinsen 1990, p. 194). Using the results in figure 8 we have for $kl = 9$ and $\beta = 157°$ that $B_{66}/\rho g b_0^2 A^2 \simeq 9.1$ for Ship 1 and $B_{66}/\rho g b_0^2 A^2 \simeq 14$ for the TPS, which in both cases gives

$$\frac{(\Omega/\omega)B_{66}}{M_{Visc}} \simeq \left(\frac{A}{1.2\ \mathrm{m}}\right)^2. \tag{7.36}$$

This means that the wave-drift damping moment exceeds the damping moment due to viscous drag for wave amplitude $A > 1.2$ m in these examples.

8. Convergence, energy balance and comparison with the translational case

Convergence properties of the induced forces computed by the low-order method employed here are discussed by Newman & Lee (1992) in the case when there is no slow motion. Convergence of the present method is illustrated here for some of the global quantities. The added mass and damping coefficients, f_{ij}^1 and $-f_{ji}^1$, should be equal, according to the theory. Computations of f_{25}^1 and $-f_{52}^1$ for Ship 1 versus the inverse number of panels $(1/N_B)$ on the wetted surface indicate in the example shown in figure 10 that $f_{25}^1 + f_{52}^1 \to 0$ as $1/N_B \to 0$. We find that $|f_{25}^1|$ and $|f_{52}^1|$ agree within a relative discrepancy of about 0.3% , and that the phase of the forces relative to 2π agrees within a discrepancy of 0.5%, for the finest discretization. Computations of the wave-drift damping coefficients B_{16} and B_{66} with various discretizations of Ship 1 demonstrate convergence, and show that quite good estimates of the wave-drift damping coefficients may be obtained by even a rather coarse discretization of the geometry (figure 11).

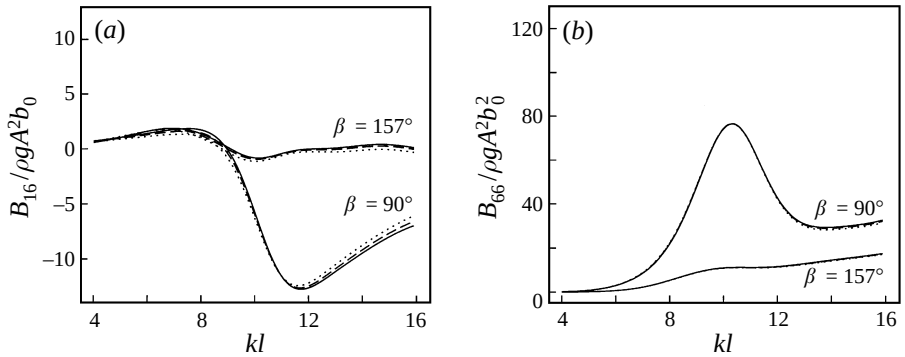

FIGURE 11. Convergence of B_{16} and B_{66} for Ship 1. Number of panels: solid line, 1600 on S_B, 6400 on S_F; dashed line, 784 on S_B, 3136 on S_F; dotted line, 400 on S_B, 1600 on S_F. $h = \infty$

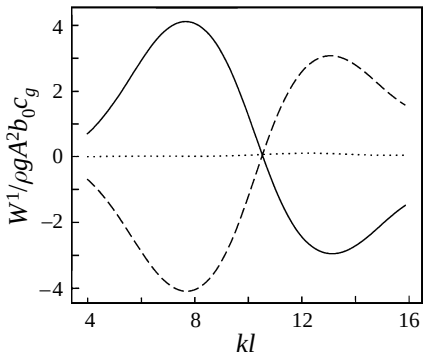

FIGURE 12. Contribution to the expression for W^1 (equation 8.2) for Ship 1, 1600 panels on S_B and 6400 panels on S_F. Solid line, the far field term; dashed line, the remaining term; dotted line, the whole expression. $h = \infty$.

It is of interest to invoke the energy equation which in one form may be written

$$\frac{\mathrm{d}(E_b + E_f)}{\mathrm{d}t} = -\int_{S_R} (p + \tfrac{1}{2}\rho \boldsymbol{v}^2 + \rho g z)\boldsymbol{v} \cdot \boldsymbol{n} \mathrm{d}S \tag{8.1}$$

expressing that the rate of change of kinetic plus potential energy of the floating body (E_b) and the fluid (E_f) inside the control surface S_R is equal to the energy flux at S_R. Let us consider the time-averaged energy equation. The difference

$$W = -\overline{\int_{S_R} (p + \tfrac{1}{2}\rho \boldsymbol{v}^2 + \rho g z)\boldsymbol{v} \cdot \boldsymbol{n} \mathrm{d}S} - \overline{\frac{\mathrm{d}(E_b + E_f)}{\mathrm{d}t}} \tag{8.2}$$

should then be equal to zero in the numerical model. Expanding W as $W = W^0 + \epsilon W^1 + \ldots$, we develop formulae for W^0 and W^1 in Appendix C. The quantity W^1 is expressed by an integral over the wetted body surface, plus terms due to the time-averaged second-order motion of the floating body, expressing the rate of change of the potential energy of the body and the fluid with respect to the wave angle, and finally a contribution involving far-field amplitudes of the potentials. We have investigated the energy balance for several geometries and find that it is satisfied to a good accuracy in all cases; an example is shown in figure 12.

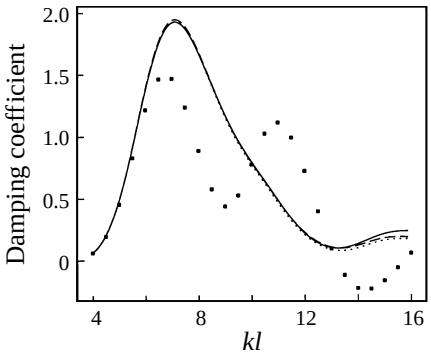

FIGURE 13. Comparison of the wave-drift damping coefficients B_{11}, B_{16} and B_{66} for Ship 1, 1568 panels on S_B, S_F. The ship is moving as described in § 8. Head waves. Solid line, $B_{11}/\rho g A^2 b_0$; dashed line, $B_{16}/\rho g A^2 sK b_0$; dotted line, $B_{66}/\rho g A^2 s^2 K b_0$; black squares, $B_{11}/\rho g A^2 b_0$ computed from Aranha's formulae. $h = \infty$.

By letting the body rotate about an axis at a large distance s, the slow motion becomes effectively unidirectional. In this case we expect to recover the results due to a slow translatory velocity of the body. In an example Ship 1 is rotating about an axis located at $x = 0$, $y = s = 100l$ away from the ship. We compare computations for head waves of B_{16}/sK obtained by (7.21) and B_{66}/s^2K obtained by (7.34), which should coincide with this scaling, approximately. (The only difference should be due to the very slow rotation about the vertical axis of the ship.) We also compare with the wave-drift damping coefficient B_{11}, i.e. the x-component of the wave-drift damping force due to slow speed in the x-direction. The latter is obtained by the method of Nossen *et al.* (1991, equation 68). The results show that the three completely different formulae give approximately the same scaled wave-drift damping coefficient, in this example, see figure 13.

Recently, Aranha (1996) has studied wave effects on a floating body with slow unidirectional speed in deep water, and has proposed a simplified formula for the far-field amplitude H^U of the linear outgoing wave, his formula (18*a*). Introducing this formula into the formulation of Nossen *et al.* (1991), he then proposes a simplified formula for the mean drift force, and thereby the wave-drift damping coefficient B_{11}, his formula (4). It is of interest to compare results using his and our formulae for the translatory problem, which may be recovered by the present formulation (see also Nossen *et al.* 1991). First we consider examples of the linear far-field amplitude, H^U. Our† and his agree for zero speed, thus we subtract the zero speed value, i.e. $H^U - H^0 \equiv (U\omega/g)H^{1U}$, and neglect terms proportional to $O(U^2)$. The geometries

† When the body is located at a position at $y_0 \to -\infty$ (and $x_0 = 0$) such that $-\Omega y_0 \to U$, the rotation of the body with respect to the origin corresponds to a translation with speed U along the x-direction. Then

$$\Omega\chi_6 \to U\chi_1, \quad \Omega\frac{\partial}{\partial\theta} \to U\frac{\partial}{\partial x}, \quad \Omega\frac{\partial\phi^0}{\partial\beta} \to \mathrm{i}kU\cos\beta\phi^0, \quad \Omega G^1 \to -2\mathrm{i}KU\frac{\partial^2 G^0}{\partial x\partial K}.$$

The fluid velocity is then given by $\boldsymbol{v} = -U\boldsymbol{i} + \nabla\Phi'$, where

$$\Phi' = \mathrm{Re}[(\mathrm{i}Ag/\omega)\phi\mathrm{e}^{\mathrm{i}\omega t}] + U\chi_1 + \psi^{(2)}, \quad \phi = \phi^0 + \tau(U)\phi^{1U}, \quad \tau(U) = \omega U/g.$$

Integral equations for the slow forward speed potentials may be deduced from the integral equations in § 5, following the procedure in GP, § 5 for the diffraction problem, and we arrive at the same results as in Nossen *et al.* (1991). Our H^U is then obtained by the integrals in Nossen *et al.* (1991, equations 64, 70, 71).

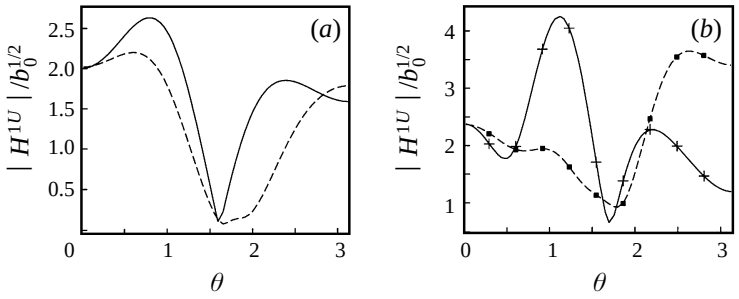

FIGURE 14. The far-field amplitude function H^{1U} for Ship 1 in translatory motion vs. polar angle θ ($0 < \theta < \pi$), computed by the complete theory (solid line), and Aranha's formulae (dashed line). Head waves. $h = \infty$. Computations with 1600 panels on S_B, 6400 on S_F. Computations with $N_B = 784$, $N_F = 3136$, are indicated with plus symbols (complete theory), and black squares (Aranha's formulae). (*a*) $kl = 6$. (*b*) $kl = 8$.

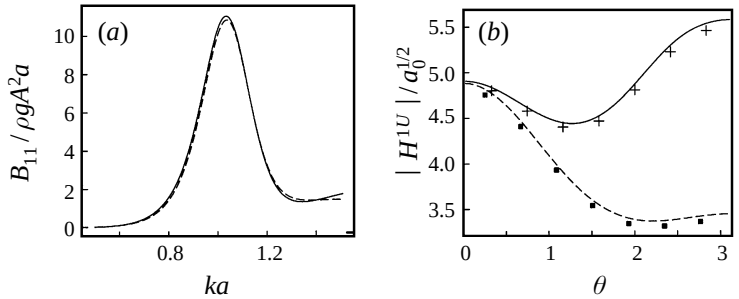

FIGURE 15. A half-immersed sphere with diameter $2a$, 784 panels on S_B and 1792 panels on S_F, in head waves: (*a*) B_{11}; (*b*) the far-field amplitude function H^{1U} for translatory motion vs. polar angle θ at $ka = 0.9$. Complete theory (solid line), Aranha's formulae (dashed line). $h = \infty$. Computations with $N_B = 400$, $N_F = 880$, are indicated with plus symbols (complete theory), and black squares (Aranha's formulae).

used are Ship 1 and a hemisphere, which both may respond freely to the waves. The computations show, however, a fundamental disagreement between our method and his proposed formula for H^U, for both geometries, see figures 14 and 15(*b*), and we question Aranha's mathematical deductions. Convergence tests are also run for the comparisons, see figures 14(*b*) and 15(*b*). (There is close agreement for $\theta = 0$, i.e. the polar angle in the opposite direction of the incoming waves ($\beta = \pi$).)

Next we consider comparisons of the wave-drift damping coefficient B_{11}. In the case of the ship there is bad agreement with Aranha for non-dimensional wavenumber larger than about 6, see figure 13. We have also performed computations for other geometries (ships) and find in general bad agreement between our and his formulae. This conclusion is also true for a restrained ship (the diffraction problem). However, as noted by Aranha, his formula give a quite good prediction of B_{11} for a floating hemisphere, as recomputed in figure 15(*a*), despite our method and Aranha's formulae leading to different H^{1U} in this example. Agreement for B_{11} is also good for an array of restrained vertical circular cylinders, as first noted by Clark, Malenica & Molin (1993).

The fundamental differences between a complete formulation of the small forward speed problem and Aranha's proposed formulae for H^{1U} and B_{11} should be looked into in more detail in future work. Likewise, the result that the two different far-field amplitudes H^{1U} in figure 15(*b*) produce approximately the same B_{11} in the case of

the floating hemisphere (figure 15*a*) should be explained, which is another topic for future investigations.

9. Conclusion

We have considered the complete radiation–diffraction problem due to a floating body performing a rotation about the vertical axis in incoming waves. The rotation angle may be an arbitrary slowly varying function of time. The mathematical problem is formulated in a relative frame of reference following the slow rotation of the body, accounting for non-Newtonian forces (the Coriolis force). First, the radiation problem coupled to the slow yaw motion of the body is formulated. Among some new features is that the usual m_j-terms in the present case include some new components. Thereafter is shown how the various components of the velocity potential may be obtained as solutions of integral equations. The mathematical problem is formulated consistently to second order in the wave amplitude and to first order in the slow angular velocity of the body. Therefore, we need also to account for time-averaged second-order velocities in the fluid which are forced by inhomogeneous boundary conditions at the mean position of the free surface and the body surface.

The linear forces and motions induced by incoming waves are considered next. The exciting forces are obtained by both pressure integration and generalized Haskind relations, accounting for the slow rotation of the body. The added mass and damping obey generalized Timman–Newman relations. Both the latter and the generalized Haskind relations are deduced from precise mathematical arguments, and are valid for geometries of arbitrary shape that are wall-sided at the water line. The linear body responses are obtained from the equation of motion, and we find that their frequencies of oscillation may in general be different in the different modes of motion. Even the frequency of the exciting force and the response in the same mode may differ in general.

The ultimate goal has been to complement a method for obtaining the complete wave-drift damping matrix for bodies of general shape, based on a panel method. The wave-drift damping coefficients are expressed by the far-field amplitudes of the linear radiation–diffraction potentials, and for B_{16}, B_{26}, by the far-field dipole moments of the velocity potential $\psi^{(2)}$, and, for B_{66}, contributions due to linear body responses coupled by the matrix (6.24) representing the effect of the Coriolis force and the restoring force matrix, see (7.21) and (7.34). These formulae are easy to evaluate once the various components of the velocity potential are determined. The method is implemented in a computer code suitable for computations on e.g. a work station. Numerical examples are obtained for the global quantities due to two different ships. Quite accurate predictions may be achieved by applying about 800 quadrilaterals on the ship surface and about 3000 on the free surface, discretized out to an outer circle with a radius of one ship length. The wave-drift damping moment is always positive in the present computations for the two ship models. We note, however, that B_{66} may in some cases become negative for arrays of vertical cylinders, see Grue (1996). The computations show that the damping forces B_{16} and B_{26} may become both positive and negative. We have invoked the energy balance in the model, finding that this is satisfied to a good accuracy.

When the rotation axis is moved far away from the body, the slow motion becomes effectively unidirectional, and results of the translational case are recovered. In this connection we compare with formulae proposed by Aranha (1996), finding a fundamental disagreement between our method and his, however. This is true both for

the coupled radiation–diffraction problem and for the pure diffraction problem, the details are explained in § 8. However, Aranha's formula for the wave-drift damping coefficient in the surge mode of motion gives a quite good prediction for a floating hemisphere and for an array of fixed vertical circular cylinders (Clark *et al.* 1993).

This work was conducted under the Joint Industry Project 'The complete wave drift damping matrix and applications'. We gratefully acknowledge the financial support from Det Norske Veritas, Mobil, Norsk Hydro and Statoil. The WAMIT radiation-diffraction program was provided by Massachusetts Institute of Technology and Det Norske Veritas.

Appendix A. The potentials in the diffraction problem

We briefly describe the potentials in the diffraction problem, outlined by GP, for completeness. The potential ϕ_D is expanded as $\phi_D = \phi_D^0 + \epsilon\phi_D^1$, $\phi_D^0 = \phi^I + \phi_7^0$,$\phi_D^1 = \phi_7^{11} + \phi_7^{12} + \phi_7^{13}$. Here, ϕ_D^0 satisfies $-K\phi_D^0 + \phi_{D,z}^0 = 0$ at the free surface and $\phi_{D,n}^0 = 0$ at the body boundary. Furthermore, ϕ_7^{11} and ϕ_7^{12} satisfy

$$-K\phi_7^{11} + \phi_{7,z}^{11} = 2\mathrm{i}K\phi_{D,\beta}^0, \qquad -K\phi_7^{12} + \phi_{7,z}^{12} = 2\mathrm{i}K\phi_{D,\theta}^0 \quad \text{at} \quad z = 0, \tag{A 1}$$

$$-K\phi_7^{13} + \phi_{7,z}^{13} = -2\mathrm{i}K\nabla_h\phi_D^0 \cdot \nabla_h\chi_6 - \mathrm{i}K\phi_D^0\nabla_h^2\chi_6 \quad \text{at} \quad z = 0, \tag{A 2}$$

$$\phi_{7,n}^{11} = 0, \qquad \phi_{7,n}^{12} + \phi_{7,n}^{13} = 0 \quad \text{at} \quad S_B. \tag{A 3}$$

The potentials ϕ_7^{11} and ϕ_7^{12} may be expressed as ϕ_D^0 by $\phi_7^{11} = 2\mathrm{i}K\phi_{D,K\beta}^0$, $\phi_7^{12} = 2\mathrm{i}K\phi_{D,K\theta}^0$. The far-field amplitudes of ϕ_7^0 and ϕ_7^{13} read, respectively,

$$4\pi H_7^0 = -\int_{S_B}\phi_7^0 h_{,n}^0 \mathrm{d}S \tag{A 4}$$

$$4\pi H_7^{13} = -\int_{S_B}(\psi_7^1 h_{,n}^0 \mathrm{d}S - 2\mathrm{i}K\phi_{7,K}^0 h_{,\theta n}^0)\mathrm{d}S + \int_{S_F}\phi_7^0 L_h(h^0, \chi_6)\mathrm{d}S, \tag{A 5}$$

where in the finite-depth case h^0 given by (5.13).

Appendix B. Remarks on the numerical implementation

The set of integral equations are solved by means of a low-order panel method (an extension of WAMIT). The body surface and the free surface are discretized by quadrilaterals (panels), and the potential or source strength is taken as constant at each panel. The Green function G^0 and its derivatives (G^1) involved in the integral equations have singularities $\nabla(1/r)$, $\nabla(1/r_1)$, $1/r$, $1/r_1$, where $r = |\boldsymbol{x} - \boldsymbol{x}'|$ and $r_1 = [(x-x')^2 + (y-y')^2 + (z+z')^2]^{1/2}$. The singularities are integrated separately over each panel by analytical methods. Numerical integration is otherwise performed using the midpoint rule.

Appendix C. Conservation of energy

From (8.2) we have

$$W = -\overline{\int_{S_R}(p + \tfrac{1}{2}\rho\boldsymbol{v}^2 + \rho g z)\boldsymbol{v}\cdot\boldsymbol{n}\mathrm{d}S} - \overline{\frac{\mathrm{d}(E_b + E_f)}{\mathrm{d}t}}. \tag{C 1}$$

Now,

$$-\overline{\int_{S_R}(p + \tfrac{1}{2}\rho\boldsymbol{v}^2 + \rho g z)\boldsymbol{v}\cdot\boldsymbol{n}\mathrm{d}S} = \frac{\rho g^2 A^2}{2\omega}\int_{S_R}\mathrm{Re}\{(\mathrm{i}\phi - \epsilon\phi_{,\beta})\phi_{,n}^*\}\mathrm{d}S. \tag{C 2}$$

Using that $\overline{\mathrm{d}(E_b+E_f)/\mathrm{d}t} = -\Omega\overline{\partial(E_b+E_f)/\partial\beta}$, we may show

$$-\overline{\frac{\mathrm{d}}{\mathrm{d}t}E_b} = \frac{\epsilon\omega}{4}\frac{\partial}{\partial\beta}\left[\omega^2\xi_i^0\xi_j^{0*}M_{ij} - m_b g\{(|\xi_4^0|^2+|\xi_5^0|^2)Z_G - 2\mathrm{Re}[\xi_6^0(\xi_4^{0*}X_G+\xi_5^{0*}Y_G)]\}\right], \tag{C 3}$$

$$-\overline{\frac{\mathrm{d}}{\mathrm{d}t}E_f} = \epsilon\frac{\partial}{\partial\beta}\left[\frac{\rho g^2A^2}{4\omega}\left(\int_{S_B}\mathrm{Re}\{K\boldsymbol{B}^0\cdot\boldsymbol{n}\phi^{0*}\}\mathrm{d}S + 2\int_{S_F}K|\phi^0|^2\mathrm{d}S + \int_{S_R}Re\{\phi^0\phi_{,n}^{0*}\}\mathrm{d}S\right)\right.$$
$$\left. + \frac{\rho g\omega}{4}\left(\int_{S_B}|B_3^0|^2n_3\mathrm{d}S + (|\xi_4^0|^2+|\xi_5^0|^2)Z_BV_B - \mathrm{Re}\{2\xi_6^0(\xi_4^{0*}X_B+\xi_5^{0*}Y_B)V_B\}\right)\right], \tag{C 4}$$

where (X_B, Y_B, Z_B) denotes the centre of bouyancy of the body and V_B the displaced volume. Expanding $W = W^0 + \epsilon W^1$ we find

$$\frac{W^0}{\rho gA^2c_g} = -\frac{1}{C_g}\mathrm{Im}\int_{S_R}\phi^0\phi_{,n}^{0*}\mathrm{d}S, \tag{C 5}$$

$$\begin{aligned}\frac{W^1}{\rho gA^2c_g} = \frac{1}{C_g}\Bigg\{&-\frac{K}{\rho A^2}\frac{\partial}{\partial\beta}\mathrm{Re}\{\xi_6^0(\xi_4^{0*}(\rho V_BX_B - m_bX_G) + \xi_5^{0*}(\rho V_BY_B - m_bY_G))\}\\
&+\frac{K}{2\rho A^2}\frac{\partial}{\partial\beta}(|\xi_4^0|^2+|\xi_5^0|^2)(\rho V_BZ_B - m_bZ_G) + \frac{K^2}{2\rho A^2}\frac{\partial}{\partial\beta}(\xi_i^0\xi_j^{0*})M_{ij}\\
&+\int_{S_B}\mathrm{Re}\{K\boldsymbol{B}^0\cdot\boldsymbol{n}(\phi_{,\beta}^0 - \mathrm{i}(\phi_7^{11} + K(\xi_{j,\beta}^0/A)\phi_j^{11}))^*\}\mathrm{d}S + \frac{1}{2}\frac{\partial}{\partial\beta}\int_{S_B}K|B_3^0/A|^2n_3\mathrm{d}S\\
&-\int_0^{2\pi}\mathrm{Re}\left[KH^0\left(\frac{C_g}{K}\tilde{H}^1 + \frac{\mathrm{i}}{C_g}\frac{\partial C_g}{\partial k}H_{,\theta}^0 - 2\mathrm{i}C_g(H_{7,K\beta}^0 + K(\xi_{j,\beta}^0/A)H_{j,K}^0)\right)^*\right]\mathrm{d}\theta\\
&-\mathrm{Re}\left[\left(\frac{2\pi}{k}\right)^{1/2}\mathrm{e}^{\mathrm{i}\pi/4}K\left(\frac{C_g}{K}\tilde{H}^1 + \frac{\mathrm{i}}{C_g}\frac{\partial C_g}{\partial k}H_{,\theta}^0 - 2\mathrm{i}C_g(H_{7,K\beta}^0 + K(\xi_{j,\beta}^0/A)H_{j,K}^0)\right)^*\right]\\
&+K\left(\frac{1}{k}+\frac{1}{C_g}\frac{\partial C_g}{\partial k}\right)\mathrm{Re}\left\{\mathrm{i}\left(\frac{2\pi}{k}\right)^{1/2}\mathrm{e}^{\mathrm{i}\pi/4}H_{,\theta}^{0*}\right\}\Bigg\},\end{aligned} \tag{C 6}$$

where $c_g = \partial\omega/\partial k$ and $\tilde{H}^1 = 2\mathrm{i}K(H_{,\beta K}^0 + H_{,\theta K}^0) + H^{13}$. For a floating body we have $\rho V_B = m_b$, $X_B = X_G$, $Y_B = Y_G$. Then the first term in the brackets on the right of (C 6) vanishes.

REFERENCES

Aranha, J. A. P. 1996 Second-order horizontal steady forces and moment on a floating body with small forward speed. *J. Fluid Mech.* **313**, 39–54.

Clark, P. J., Malenica, S. & Molin, B. 1993 An heuristic approach to wave drift damping. *Appl. Ocean Res.* **15**, 53–55.

Emmerhoff, O. J. & Sclavounos, P. D. 1992 The slow-drift motion of arrays of vertical cylinders. *J. Fluid Mech.* **242**, 31–50.

Emmerhoff, O. J. & Sclavounos, P. D. 1996 The simulation of slow-drift motions of offshore structures. *Appl. Ocean Res.* **18**, 55–64.

Faltinsen, O. M. 1990 *Sea Loads on Ships and Offshore Structures.* Cambridge University Press.

Grue, J. 1996 Interaction between waves and slowly rotating floating bodies. In *Waves and Nonlinear Processes in Hydrodynamics* (ed. J. Grue, B. Gjevik and J. E. Weber). Festschrift for Professor Enok Palm on his seventieth birthday, pp. 71–82. Kluwer.

Grue, J. & Biberg, D. 1993 Wave forces on marine structures with small speed in water of restricted depth. *Appl. Ocean Res.* **15**, 121–135.

Grue, J. & Palm, E. 1993 The mean drift force and yaw moment on marine structures in waves and current. *J. Fluid Mech.* **250**, 121–142.

Grue, J. & Palm, E. 1996 Wave drift damping of floating bodies in slow yaw motion. *J. Fluid Mech.* **319**, 323–352 (referred to herein as GP).

Huijsmans, R. H. M. & Hermans, A. J. 1985 A fast algorithm for computation of 3-D ship motions at moderate forward speed. *4th Intl Conf. on Numerical Ship Hydrodynamics.*

Malenica, S., Clark, P. J. & Molin, B. 1995 Wave and current forces on a vertical cylinder free to surge and sway. *Appl. Ocean Res.* **17**, 79–90.

Newman, J. N. 1977 *Marine Hydrodynamics.* The MIT Press.

Newman, J. N. 1993 Wave-drift damping of floating bodies. *J. Fluid Mech.* **249**, 241–259.

Newman, J. N. & Lee, C. H. 1992 Sensitivity of wave loads to the discretization of bodies. *Proc. 6th Intl Conf. Behaviour of Offshore Structures (BOSS '92), London, UK*, (ed. M. H. Patel and R. Gibbins), Vol. 1, BPP Technical Services Ltd.

Nossen, J., Grue, J. & Palm, E. 1991 Wave forces on three-dimensional floating bodies with small forward speed. *J. Fluid Mech.* **227**, 135–160.

Wehausen, J. V. & Laitone, E. V. 1960 Surface waves. In *Handbuch der Physik* IX.

Wichers, J. E. W. & van Sluijs, M. F. 1979 The influence of waves on the low frequency hydrodynamic coefficients of moored vessels. *Proc. Offshore Technology Conf., Houston, OTC 3625.*

Wu, G. X. & Eatock Taylor, R. 1990 The hydrodynamic force on an oscillating ship with low forward speed. *J. Fluid Mech.* **211**, 333–353.

Zhao, R. & Faltinsen, O. M. 1989 Interaction between current, waves and marine structures. *5th Intl Conf. on Num. Ship Hydrodynamics, Hiroshima.* National Academy Press, Washington DC.